THESIS

LIBRARY
Michigan State
University

3 1293 10063 4090

This is to certify that the

thesis entitled

The Nature of Infiltration Curves

presented by

Jeffrey E. Friedle

has been accepted towards fulfillment
of the requirements for

M.S. degree in Agr. Engr.

George E. Merva

Major professor

Date Nov 7, 1979

O-7639

MSU

OVERDUE FINES ARE 25¢ PER DAY
PER ITEM

Return to book drop to remove
this checkout from your record.

THE NATURE OF INFILTRATION CURVES

By

Jeffrey E. Friedle

A THESIS

Submitted to
Michigan State University
in partial fulfillment of the requirements
for the degree of

MASTER OF SCIENCE

Department of Agricultural Engineering

1979

ABSTRACT

The Nature of Infiltration Curves

by

Jeffrey E. Friedle

Infiltration tests were performed on air dry layered soil columns. Data was continously recorded using a video cassette recording system. Infiltration "curves" were generated and represented by a series of line segments when data was plotted on semi-logarithmic graph paper. Literature supports the interpretation that certain changes of slope indicate a wet front passing an interface between soil layers. Data and literature suggest that remaining slope changes between line segments may be due to the interrelationship of matrix, pressure and gravitational potential, the components of total water potential.

Approved: ______________________
Major Professor

Approved: ______________________
Department Chairman

To G. G.

ACKNOWLEDGMENTS

I would like to thank the Department of Agricultural Engineering for their financial support. To my wife Sandy, and my friends, George "Brownie" Brown, Fran Wolak, Yoosef Shahabasi, Inacio Dal Fabbro, Dorota Haman, and Howard Doss thank you for your moral support. Above all I would like to thank George E. Merva, a man who is a Christian in the true sense of the word, and has patience with no end.

TABLE OF CONTENTS

LIST OF TABLES

LIST OF FIGURES

I. INTRODUCTION

Many different approaches have been used to study the phenomena of vertical infiltration into soil. Darcy (1965) (cited by Swartzendruber (1966)). Buckingham (1907) Green and Ampt (1911), and Richards (1931) studied the physical aspects of fluid flow or the force driving the flow. This information could then be used to model vertical infiltration.

Another approach, used by Horton (1940) and his contemporaries, was to define infiltration not from the physical aspects of the actual phenomena but rather from the after effects, namely the runoff. The gross approximation of "rainfall minus runoff equals infiltration" was adjusted to attempt to account for evaporation, storage, and detention. With the realization that this method would at best give areal infiltration the researchers directed their attention to fitting curves mathematically to existing data.

With the improvement of mathematical techniques and development of computers a new approach evolved. This is a refinement of the "physical aspects" era. "Philip, (1954) Collis-George (1977) and others have refined and extended the work of Darcy, Buckingham, Green & Ampt, and Richards.

While reflecting on these different approaches, I noticed a similarity in the shape of an infiltration curve and the recession limb of a runoff hydrograph. I applied Barnes' (1940) method of hydrograph separation to some infiltration data of Musgrave & Free (1936). The resulting graph on semi-logrithmic paper was not a curve but appeared to be four straight lines. This incident prompted me to initiate the following work. The objectives of my study are to:

1. Review the literture to determine if any infiltration models account for the several straight lines observed.

2. Obtain infiltration data that will show instantaneous rates and changes of the instantaneous rate.

3. Determine the possible cause of the straight lines when infiltration is plotted as the log of flow rate versus time.

II. LITERATURE REVIEW

The accurate prediction of runoff and the optimization of irrigation rate rely on some method of estimating the volume and rate of water infiltrated into the soil. The popularity of developing mathematical models describing rate of volume of infiltration has been cyclical since Darcy first published his equations for saturated flow in 1865. Some work was done in the early 1900's. A real flurry of interest however, started in the late "30's" and early 1940's. A background level of model development was maintained until the mid "50's" when, mathematical refinements intensified interest again. Since the rekindling of interest in this area of work, many people have added their thoughts to the subject.

I will review the work done in model development of infiltration in chronological order. Similarities of idependently developed models, and how one model may be the second generation of a previously published equation will be shown.

Darcy (1865) (cited by Swartzendruber (1966)) developed a theoretical physically based equation for saturated flow through a sand filter. Water was ponded on the filter, and flow was assumed to be steady and the medium homogeneous. He defined the volume flow rate as:

$$Q = -Ka\Delta h/L \qquad (1)$$

K = Water transport constant
A = Area
$-\Delta h$ = hydraulic head difference
L = Length

Buckingham (1907) extended Darcy's model to include unsaturated flow. With a homogeneous medium, Buckingham expressed his model in two forms. Using either capillary potential, or the water content gradient the flux is:

$$Q = \lambda \partial\psi/\partial\chi = \lambda\partial\psi/\partial\theta \cdot \partial\theta/\partial\chi \qquad (2)$$

Q = Flux
θ = Water Content
λ = Cappillary Conductivity
ψ = Water Potential
χ = Distance

Green and Ampt (1911) based their work on Poiseuille's law. They assumed the soil was a bundle of cappillary tubes irregular in shape and length. For a homogeneous soil with a ponded surface and uniform initial water content Green & Ampt related the depth of water penetration to time. For vertical infiltration:

$$(P/S) \cdot (t) = \ell - (a+k) \times \log\,(1 = \ell/(a+k)) \qquad (3)$$

S = Porosity
P = Permeability
t = Time
ℓ = Distance water has penetrated
a = Depth of water on soil surface
k = Capillary potential at wet front

Smith (1975) has shown a more convenient form of the Green and Ampt model to be:

$$f = K_s\ (H_c + L + d)/L \qquad (3a)$$

f = Infiltration rate
K_s = Effective conductivity
H_c = Capillary tension across wet front
d = Surface depth of water
L = Length

Smith has also shown, for small values of time, the infiltration rate approaches:

$$f = K_s + 2\ \theta c(H_c+d)/K_s \cdot t^{-\frac{1}{2}} \qquad (3b)$$

where θ_c is the initial empty volume (available porosity).

Gardner and Widstoe (1921), used Buckingham's model and the equation of continuity to obtain an equation analogous to the diffusion equations. From experimental evidence they assumed that for a large number of soils, the capillary potential was a linear function of the reciprocal of the mositure density. They used the relation:

$$\psi_c = -\frac{c}{\rho} + b$$

where ρ is the moisture density, c and b are constants. The model for vertical infiltration in homogeneous soil is:

$$\chi = c_1 t + c_2 \left(1-e^{-Bt}\right) \tag{4}$$

χ = depth
t = time
c_1, c_2, B = constants

Gardner and Widstoe's (1921) equation (4) can be expressed as a rate equation:

$$f_t - f_\infty + (f_o - f_\infty) \; e^{-Bt} \tag{4a}$$

f_t = infiltration at time t (rate)
f_o = infiltration at time o (rate)
f_∞ = infiltrationat time ∞(rate)
t = time
B = constant

Rather than write the flow equation in terms of water content as Gardner & Widstoe (1921) had done Richards (1931) wrote the flow equation in terms of the capillary potential:

$$\frac{\partial\theta}{\partial t} = \nabla\cdot K \, \nabla\Phi \tag{5}$$

Θ = water content (volumetric)
t = time
K = capillary conductivity
Φ = total potential

Richards also measured capillary conductivity, and showed it was a function of capillary potential and water content. Gardner (1967) pointed out that the functional dependence of capillary conductivity on the capillary potential is what makes Richards' model difficult to solve. In order to simplify the solution, the diffusion equation with a constant diffusion coefficient was applied to water movement. It turns out, however, that the assumption of a constant diffusion coefficient is not justified (Kirkham & Feng (1949) as cited by Gardner (1967)).

Kostikov (1932), derived an empirical model for a homogeneous soil. This model relates hydraulic conductivity for air-dry soil to the hydraulic conductivity for saturated soil. The exponential relation is:

$$K_o = K_D \cdot T^{\alpha} \tag{6}$$

K_o = hydraulic conductivity air dry soil
K_D = hydraulic conductivity saturated soil
α = constant
T = time
(subscript D is for Darcy)

The model for infiltration usually associated with Kostiakov can be derived from this expression, but did not appear in the literature until five years later. Lewis (1937) (cited by Swartzendruber & Huberty (1958)) published the model for cummulative infiltration:

$$i = kt^{\alpha} \tag{6a}$$

i = cummulative infiltration
α,k = constant
t = time

This model is particularly easy to use and has found acceptance with many people. Horton (1940) did not like the model because the differentiated form implies an initial rate of infinity, and a final rate of zero. Philip (1957) has shown that alpha (α) and k are not constant but vary with time. Alpha at small times is equal to ½, and for large times alpha approaches one, and K approaches the saturated hydraulic conductivity of the material.

Horton became involved in the development of a model that would describe the infiltration process, because he was interested in the runoff phenomona. Horton (1940) described infiltration as an exhaustive process, "the rate of performing work is proportional to the amount of work remaining to be performed". With this in mind, Horton empiricaly proposed a model:

$$i = f_c t + ((f_o - f_c) / K) \cdot (1 - e^{-Kt}) \qquad (7)$$

i = cummulative infiltration
f_c = steady state infiltration rate
f_o = initial infiltration rate
K = constant

Hortons model has a striking resemblence to the Gardner and Widstoe model of 1921. Letting $i = x$ the two models are the same assuming $c_1 = f_c$, $c_2 = (f_o - f_c)/k$ and $\beta = K$. The only difference between the models is Horton's interpretation of the constants, as physical parameters of the soil. These models have the advantage of approaching a constant rate as time goes to infinity. Philip (1957) fit Horton's equation using laboratory date. Philip found that the equation had considerable error compared to the data for cummulative infiltration. When Horton's model was fit to field data, Skagges et al (1969) found a close fit. Watson (1959) postulated that Philip's poor fit may have been due to the ability of entrapped air to escape from the coil column in the laboratory situation. Both Watson (1959) and Collis-George (1977) noted that the Horton equation does not fit exactly at very short times when the rate is changing very rapidly. Both authors however show the equation fits well for intermediate and long times.

Philip developed several models for infiltration into a homogeneous soil with a uniform initial moisture content. Philip's (1954) model is the same form as proposed by Green and Ampt (1911) with two assumptions. Philip assumed (reported by Gardner (1967)) that the diffusivity at the initial water content is zero, and at water contents greater than the initial, diffusivity is infinite. Philip's (1954) model is:

$$t = y\,(F - B \log (F/B)) \qquad (8)$$

Collis-George (1977) found that the Green & Ampt form equations failed at long times. Skagges et al (1969) noted that these types of models underpredicted infiltration rate at long times. Philip's second model derived for a homogeneous soil, uniform initial water content, and a ponded surface is more general than his first. Using a numerical technique, Philip (1957) solved the general flow equation to obtain an algebraic expression for cumulative infiltration:

$$i = St^{\frac{1}{2}} + At \qquad (9)$$

i = cumulative infiltration
S = constant
t = time
A = constant

Philip describes the new parameter "S", sorptivity, as the measure of capillary uptake or removal of water. Smith (1975) for short times expressed Green & Ampt's model (equation 3) in the same form as Philips (1957) model when differentiated.

$$F = 2St^{-\frac{1}{2}} + A \qquad (9a)$$

F = infiltration rate

Watson (1959) and Collis-George (1977) both found the Philip model to fit well at short times. Watson, however, notes that Philip's (1957) model does not predict the infiltration rate well at long times. The model underpredicts infiltration at long times.

Holtan (1961) proposed that the rate of infiltration is a function of the volume of potential storage remaining. The potential volume of infiltration F_p is some factor "K" times "S", the available porosity, above the restricting horizon in the soil. The parameter "k" is dependent on the vegative cover. Holtan claimed that $f-f_c$ plotted against F_p, the remaining potential storage, produced a straight line relation on log-log paper, thus the expression:

$$f-f_c = aF_p^{\,n} \tag{10}$$

n = constant
a = constant
f = infiltration rate
f_c = constant infiltration rate
f_p = remaining potential storage

In Holtan's paper, "a" was said to vary from 0.26 to 0.8 depending on the type of vegative cover. The constant "n" was, for all plots, 1.387. There has been some question as to what control depth to use to compute F_p, the potential storage. Skaggs et al (1969) computed a control depth from the initial soil water content, the soil porosity and the volume of water infiltrated up to the time of constant rate. They felt this method gave better results than using the depth to the B horizon as suggested by Holton and Creitz (1967) (cited by Idike et al (1977)). With this alternate method of control depth determination, Holtan's model was found by Skaggs et al (1969) to fit plot data very well (R^2 of 0.988).

Overton (1964) refined Holtan's equation by integrating Holtan's model to obtain an instantaneous infiltration function. Overton assumed n = 2 in order to integrate the function. Loss of accuracy due to the assumption of n = 2 was made up for by more accurate prediction of "a".

The resulting rate equation is:

$$f=f_c \text{ secant}^2 ((aF_c)^{\frac{1}{2}} (t_c-t)) \qquad (11)$$

f = infiltration

f_c = constant infiltration rate

t_c = time to constant rate

a = constant

Overton compared his refined Holton model algebraically with Green & Ampt, Horton, Kostiakov, and Philips' model, and found them equivalent.

Most models to this point assumed an excess of water (ponded) at the surface. Mein & Larson (1971) approached the situation slightly different. Considering the application rate could be less than the infiltration capacity they used two equations to model infiltration. A modified form of Darcy's law was used to calculate the volume of infiltration (F_s) prior to runoff.

$$F_s = S_{av} (IMD)/((I/k_s)-1) \qquad (12)$$

S_{av} = Average capillary suction at wet front
IMD = Porosity - Initial Moisture content
K_s = Saturated Hydraulic conductivity
I = Rainfall intensity

A form of the Green & Ampt equation was to model infiltration rate after runoff begins:

$$f_p=K_s(1+(S_{av}(IMD))/F) \qquad (13)$$

f_p = infiltration rate

Idike et al (1977) found that the Mein & Larson model predicted time to runoff very well and fit the data at middle and long time infiltration reasonably well.

None of the equations surveyed up to this point modeled infiltration data over the entire range of time. Some models describe short time phenomena while other models are better at describing the infiltration process from intermediate to long times. Collis-George (1977) assumed that infiltration at short times was "independent but superimposed" on the long time steady state process. Bodman & Coleman (1944) (cited by Collis-George (1977)) stated, for long times the cumulative infiltration as:

$$i = i_o + Kt \tag{14}$$

i = cumulative infiltration
i_o = a constant
K = conductivity of transmission zone

Superimposing the short term affects, f(t), the model becomes:

$$i = Kt = F(t) \tag{15}$$

Where $f(t) = i_0$ at steady state. Collis-George (1977) used Philip's (1957) approximation, $i = St^{1/2} + At$ (eq. 9) for short time infiltration. He also introduced t_c, which divides long and short times. He interrelated t_c and i_0 as:

$$i_o = S(t_c)^{1/2} \tag{16}$$

and used these parameters to normalize equation 15. Solving this normalized function Collis-George found that cumulative infiltration could be expressed:

$$i = i_o\ (\text{Tanh } T)^{1/2} + Kt \tag{17}$$

$$T = t/tc$$

All the algebraic models for infiltration presented with the exception of Holtan's and Collis-George's models are interrelated. None of the models describe infiltration data accurately over the entire range of time. Nor do they suggest the occurence of several straight lines when the method of hydrograph separation is applied to infiltration data.

Coleman and Bodman (1945) showed in layered soils there was a break in the slope of the infiltration curve, when a wet front passed the interface between layers. When infiltration rate data was plotted on logarithmic scaled graphs the slope of the infiltration curve become more negative when the wet front passed into a layer with finer pores. If the wet front passed into a layer with larger pores a decrease in the slope of the rate curve occurred. Miller and Gardner (1962) attributed the change of slope in the first case to a rapid filling of small pores, and the difficulty in transmitting water through the ever thickening layer of fine pores. Miller and Gardner explained for a wet front moving from a small to a larger pored material, the smaller pores hold water at a tension that the larger pores are unable to achieve. Infiltration rate will decrease as water "piles up" at the interface. Moisture content will increase at the interface, and at some point water will flow into some of the pores in the lower layer, and establish channels of flow.

Colman and Bodman (1945) and Miller and Gardner (1962) discussed the change in the slope due to the wet front passing the interface between textural layers. None of their data however suggests the existance of several line segments within a layer. This may be due to their lack of accurate data.

Other aspects of infiltration of interest are the concepts of total water potential and soil moisture characteristic. Water in a system flows due to a difference in water potential. Taylor and Ashcroft (1972) describe total water potential as the ability of water in a system to do work with respect to some water in a reference state. Total water potential is comprised of several components. The components of potential that this study was concerned with were:

1. Matrix potential (capillary tension)
2. Pressure potential (head)
3. Gravity potential

Moisture content is related to matrix potential. Every soil has a characteristic curve of moisture content versus matrix potential. At a given moisture content the soil will have a given total water potential (Bodman and Colman (1944)).

Bodman and Colman (1944) found in a single layer they could define four distinct zones during infiltration. Each of these zones exhibited certain properties. The first zone was a saturated zone. This zone was thin (1.5 cm) maximum and at pore space saturation in their experiments.

Below this thin saturated zone were three zones that were not saturated. The first of these was a transmission zone. Water content in the transmission zone was relatively constant and as infiltration proceeded this zone lengthened. The second unsaturated zone was the wetting zone. This zone connected the transmission zone to the wet front. The wetting zone exhibited a large change in moisture content. The last zone, the wet front, was the interface between the wetting zone and the dry soil. There was a very large moisture gradient across this wet front.

III. PROCEDURE AND APPARATUS

Infiltration data has been collected using several methods. Horton (1937) determined infiltration by subtracting measured runoff from measured rainfall. A mariotte bottle with a graduated cylinder was employed by Childs and Bybordi (1969) to measure cumulative volume of infiltration versus time. Swartzendruber and Huberty (1958) used a hook gage to measure the change in depth of ponded water with time as it infiltrated into soil. The data collected from these measurements were not an instantaneous infiltration rates, but an average rate over the time period between readings.

A system to measure the instantaneous infiltration rate and continuously record the infiltration rate and time was designed. Water was supplied from a large (approximately 19 litre) container using a mariotte (constant head) device. Two variable area flow meters were used to measure the volume flow rate of water delivered to a soil column. These flow meters provided a range of measurement of 1 ml/min to 39 ml/min[1] and 0.01 ml/min to 4.0 ml/min[2]. The Fischer-Porter flow meter could be interpolated to the nearest 0.1 ml/min. The Gilmont flow meter had four ranges of accuracy as shown in Table 1.

---

[1] Fischer-Porter Co., Warminster PA., model 448-118, stainless steel float.

[2] Roger Gilmont Inc., Great Neck, NY., model S-157.

Table 1. Ranges of Interpolation for the Gilmont Flow Meter

Flow Range (ml/min)	Interpolated to the nearest (ml/min)
0.01-0.1	0.005
0.1-0.2	0.01
0.2-1.0	0.025
1.0-4.0	0.05

The flow meters were connected in parallel, between the water supply container and the soil column. Flow could be directed to either of the meters by a three way "T" valve (see Figure 1). The Gilmont flow meter was used for flows below 4 ml/min.

The soil column was 60 cm long and 2.5 cm in diameter. Soils with the textural classifications of sand, loam, and clay[3] were used in different combination in the soil column. Before being placed in the column the soils were sieved using a #7 U.S. Standard Sieve.[4] This sieving removed organic debris, stones and clods of soil. The bottom of the soil column was blocked using a rubber stopper with a hole. A funnel with a long spout was used to fill the soil column. As the soil level rose in the soil column, the funnel was raised. This arrangement was an attempt to provide for a "flow" of soil rather than a free fall drop, to prevent particle size stratification. A two holed rubber stopper was used to close the top of the soil column. One hole was used for the water delivery tube from the flow meters and the second hole had a short

---

[3]Personal communication Ghasem Asrar, Crop & Soils Sciences Department.

[4]Sargent & Co., Chicago IL, #7, 2830 microns.

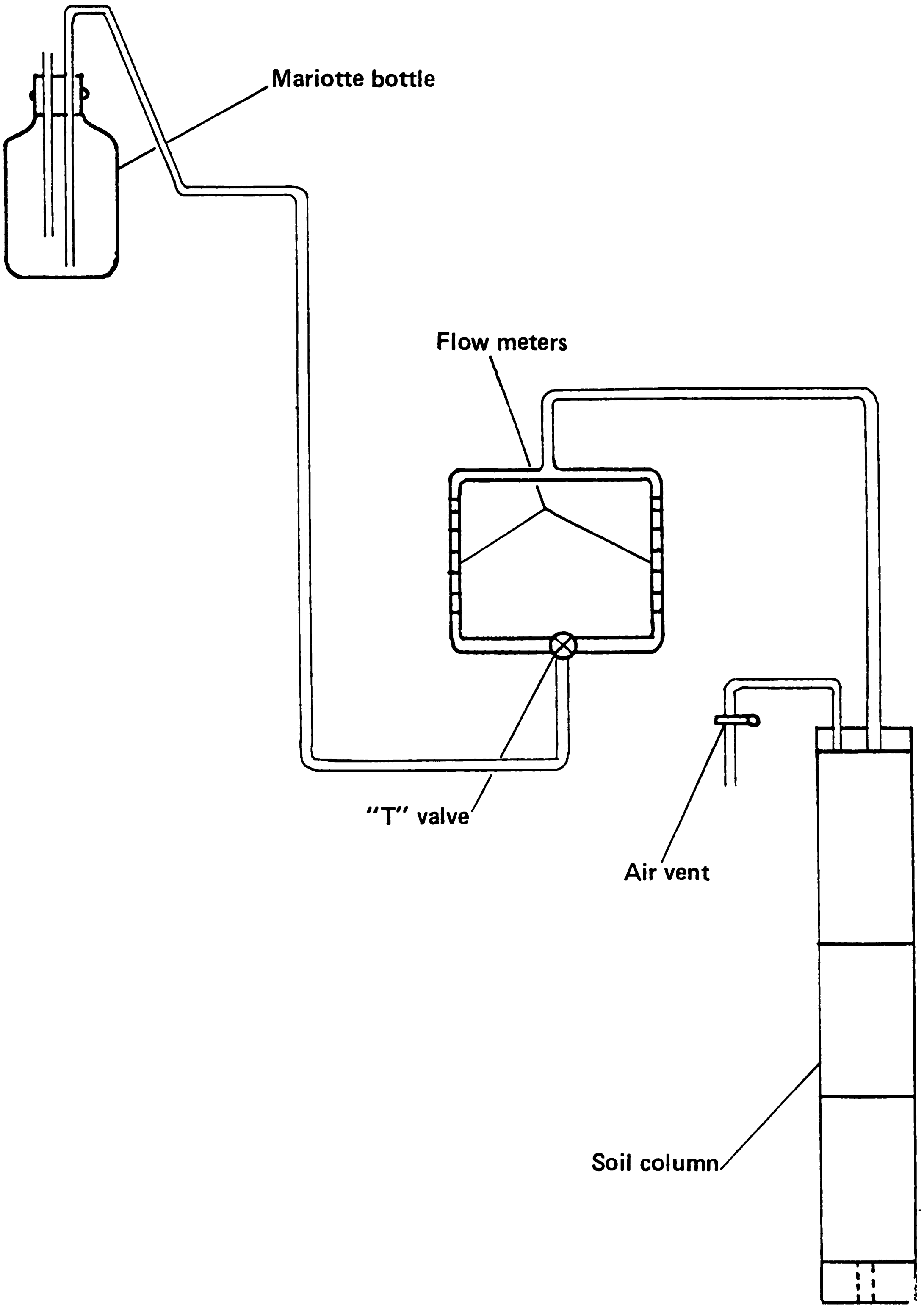

Figure 1. Arrangement of infiltration rate measuring equipment.

piece of plastic tubing with a clamp, which could be opened to let trapped air out of the system.

A digital timer[5] was used as a time reference. The timer displayed hours, minutes and seconds, including tenths and hundredths of a second. Intermediate times could be stored with the timer, and recalled at the end of the experiment.

Data from the digital timer and flow meters was continously recorded, using a black and white video cassette system.[6]

The preceeding arrangement of equipment was used to run several experiments. Water to be used for infiltration was drawn from the tap. The water was allowed to come to equilibrium temperature with the measuring equipment and soil column. This was to minimize the effect of temperature potential. The flow meters were not calibrated, because I was interested in the difference of flow rates during a particular experiment, rather than absolute flow rates. Special care was taken to eliminate air bubbles from the plastic water delivery tubing.

Hydraulic head at the soil column was changed by adjusting the mariotte device in the water supply bottle. A small positive head was maintained at the soil column. This eliminated the need to calculate head loss in the delivery tubing, valve assembly and flow meters. With the video system recording, water flow and the timer were started. The experiment was allowed to run until water dripped from the bottom of the soil column.

---

[5]Hewlett Packard Corvallis Ore., Model HP-55.

[6]Panasonic Tri-color video cassette recording deck. Sony model ACV 3200. Black and White video camer Sony 21" Trinctron Video moniter.

Video tapes of the experiments were analzyed using video tape editing equipment.[7] The video editing equipment provided frame by frame viewing, as well as stop motion. The video equipment provided 60 frames/second. The digital timer used was accurate to 1/100 second. The stop motion allowed instantaneous volume rate and time to be read from the measuring instruments. The data points obtained using the video equipment were graphed on semi-largrithmic paper. Time was graphed on the horizontal axis and the logarithem base e of flow/time was graphed on the vertical axis. See appendix for method of fitting lines.

---

[7]Tri EA5 CONSOLE , two Sony 2600 Video Recorders.

IV. RESULTS AND DISCUSSION

RESULTS

Two experiments were run, each with one replication. Experiments one and two had three layers of soil each consisting of sand, clay, and loam. Each successive layer was a soil of finer texture. Experiments three and four contained three soil layers, in a different order, loam, clay, and sand. The clay layer was a finer textured soil than the loam layer preceding it. The third soil layer of sand was a courser texture than the preceding layers of loam and clay.

Data was graphed on semi-logarithmic graph paper. Volume rate (ml/min) is the ordinate (logarithmic axis) and time (hours) the abcissa. The natural logarithm (base e) was used in computations.

Experiment one used a layer of sand 26.5 cm thick over a layer of loam 16.0 cm thick. The bottom layer of clay was 14.5 cm thick. Figure 2 is the plot of the data from experiment one. The visible wet front reached the bottom rubber stopper at 0.490 hours. Three straight line segments were fit for each layer of soil. The line segments were divided into their respective layers based on the time the visible wet front passed the soil interfaces. Table 2 gives the slopes of the line segments within the soil layers. Experiment one was stopped at 0.490 hours because the flow was below the range of the flow meter.

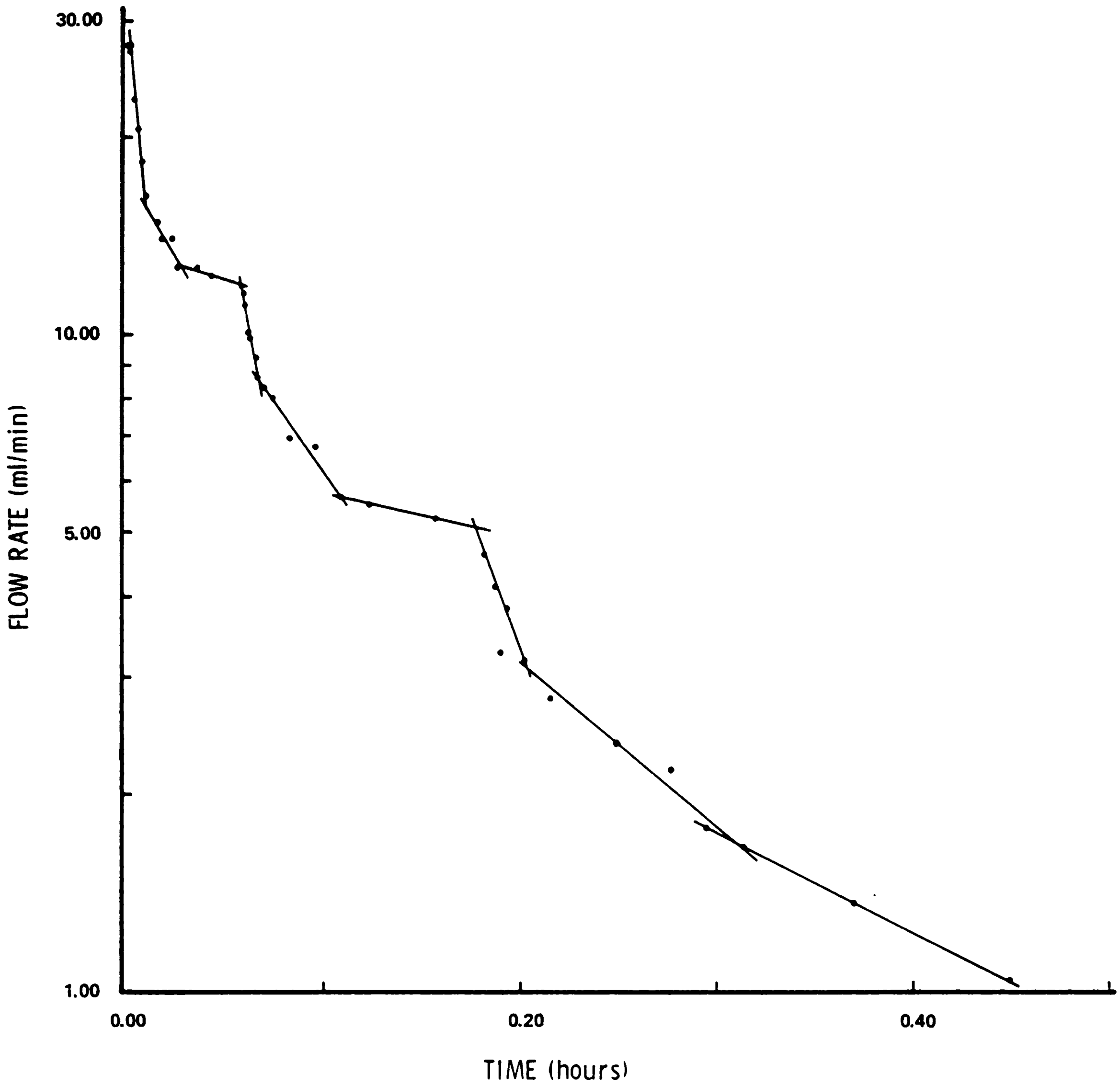

Figure 2. Semi-logarithmic plot of data from experiment one.

Experiment two had three layers of soil. The sand, loam, and clay layers were 31.5 cm, 14.5 cm, and 12.0 cm thick respectively. There was a visible discontinuity in the clay layer 2.5 cm below the loam-clay interface. This was caused by an interruption in the filling of the soil column.

The visible wet front passed the sand-loam interface at 0.136 hours, and crossed the clay interface at 0.306 hours. The wet front passed the discontinuity in the clay layer at 0.367 hours.

Figure 3 is the plot of data from experiment two. Line segments were associated with a soil layer based on the time the visible wet front passed the soil layer interfaces. There were four line segments in the sand layer (see Table 2 for slopes). Flow increased at 0.0451 hours when the head was increased from 0.0 cm to 5.0 cm. There were three line segments in the loam layer. The break in the data from 0.195 hours to 0.217 hours, was caused when flow was switched to the lower reading flow meter. I removed an air bubble from the water delivery tube, which caused an increase in flow, and a break in the data from 0.338 hours to 0.348 hours. There were four line segments in the clay layer. The time associated with the break between the first and second line segments in the clay layer at 0.39 hours was approximately the time the visible wet front passed the discontinuity in the clay layer at 0.367 hours.

Experiment three and four used soil columns composed, from top to bottom, of layers of loam, clay, and sand. Experiment three used layers of loam, clay, and sand, 10.8 cm, 8.0 cm, and 38.6 cm thick. There was a discontinuity 2.0 cm from the top of the loam layer.

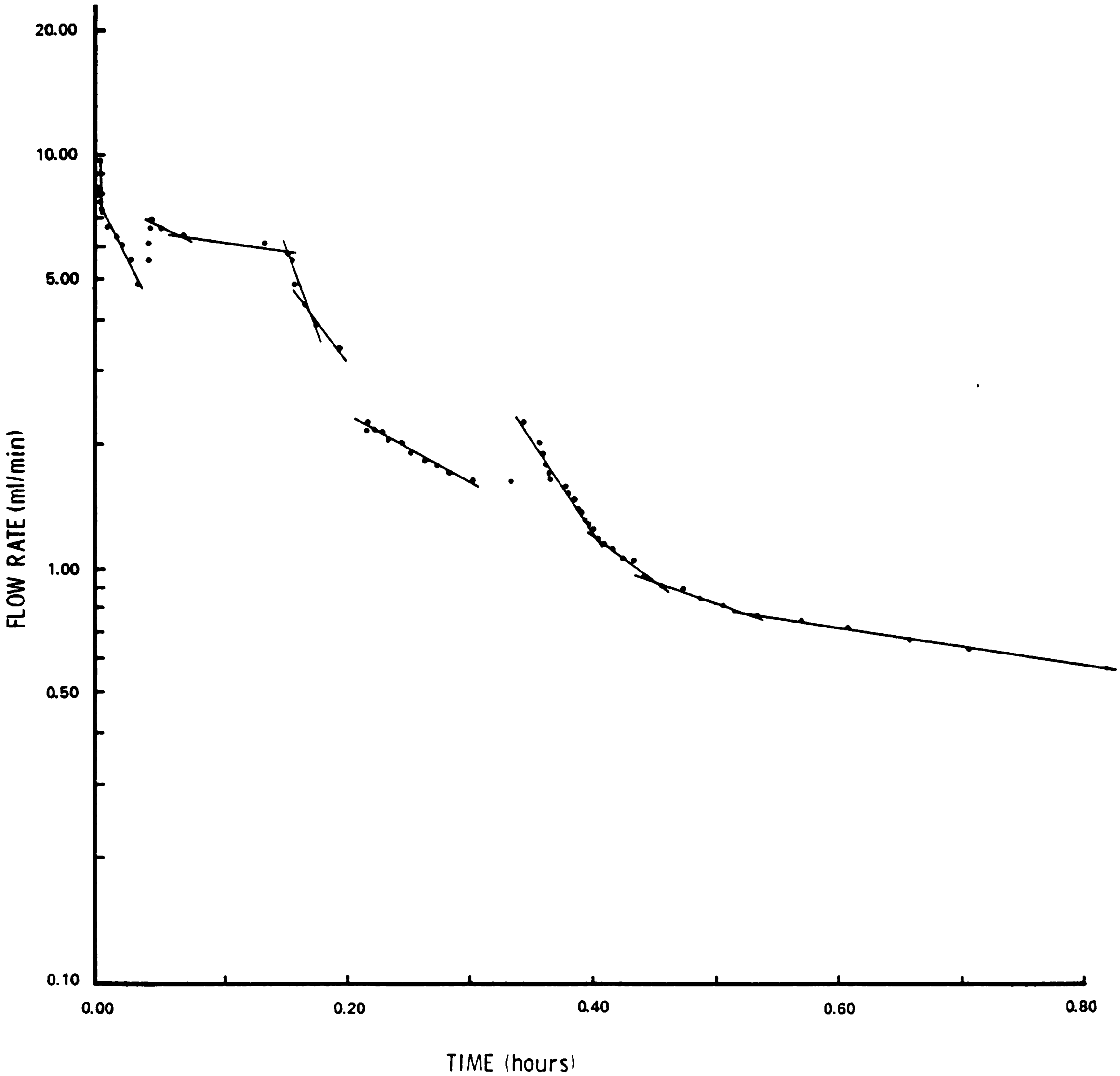

Figure 3. Semi-logarithmic plot of data from experiment two.

The visible wet front passed the loam-clay interface at 0.0640 hours and the clay-sand interface at 0.0330 hours.

The data from experiment three is plotted in Figure 4. The times at which the visible wet front passed the soil interface were used as the basis for assigning line segments to soil layers. There were four line segments in the loam layer. The break in data from 0.015 hours to 0.0240 hours was caused when flow was changed to the lower reading flow meter. The clay layer in experiment three had three line segments. There was only one line segment in the sand layer.

In experiments one, two, and in the loam and clay layers of experiment three, the visible wet front was well defined and even as it passed through the soil layers. The visible wet front in experiment three paused at the clay-sand interface. When the wet front passed the interface, it did so in channels, leaving portions of the sand dry.

Experiment four was similar to experiment three. The soil column had layers of loam, clay, and sand, 17.0 cm, 12.0 cm, and 28.5 cm thick. Due to an error on my part the exact times the visible wet front passed the soil interfaces are not available. The visible wet front passed the clay-sand interface at approximately the one-hour mark. When the visible wet front did pass the clay-sand interface, it was traveling in channels as in experiment three.

When the visible wet front, in the four experiments, crossed an interface into a soil layer with a finer texture the slope of the "curve" (line segment) became more negative. When the visible wet front in the four experiments passed into a soil layer with a coarser texture the slope of the "curve" (line segment) became less negative. These results agree with the findings of Colman and Bodman (1945) and Miller and

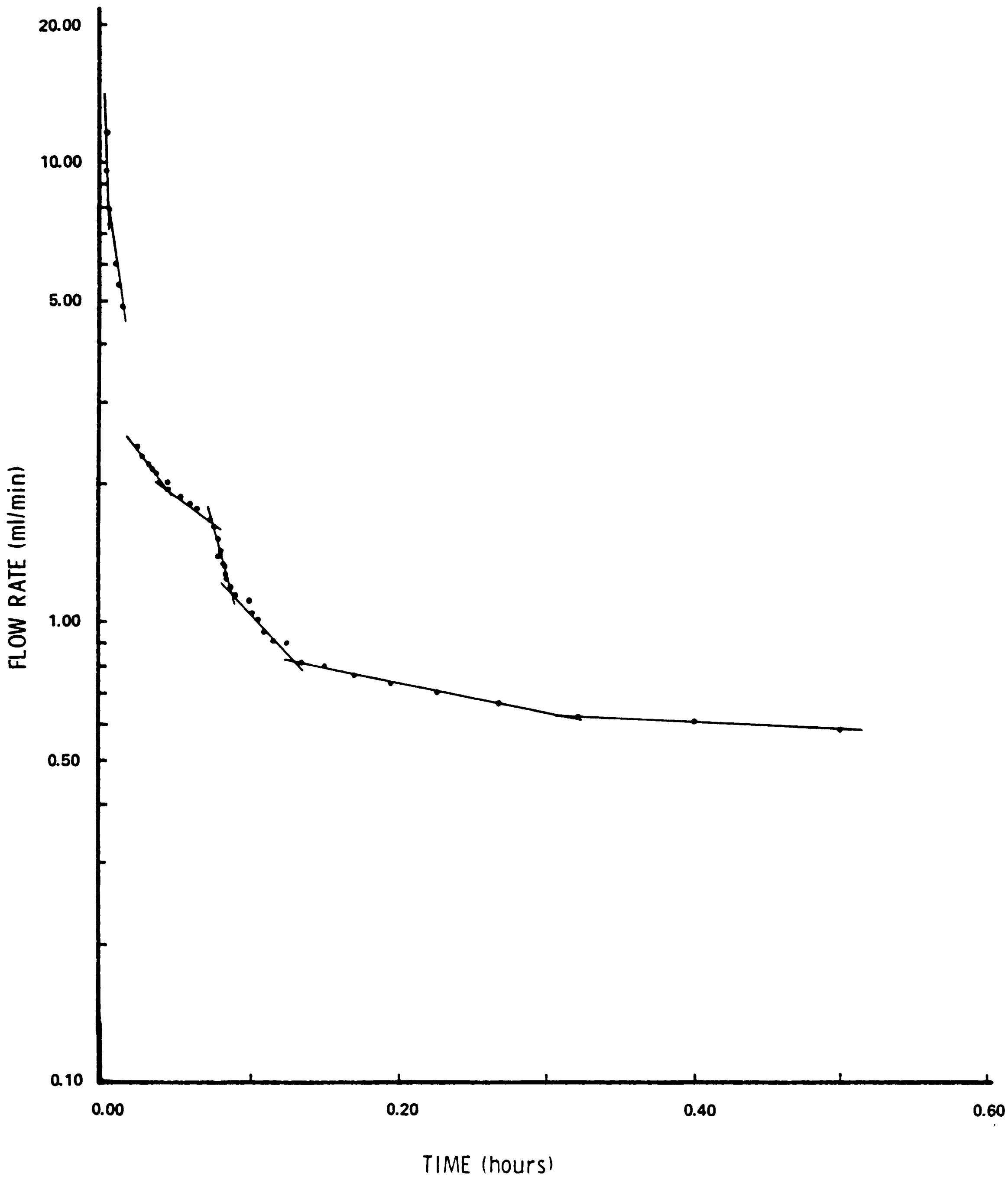

Figure 4. Semi-logarithmic plot of data from experiment three.

Table 2. Slopes of the line segments within soil layers.

Layer	Exp 1	Exp 2	Layer	Exp 3	Exp 4
Sand	-60.66	-154.00*	Loam	-102.20*	-223.99
	-14.42	-11.30*		-34.70*	-71.03
	-1.99	-3.68*		-11.20*	-12.23
		-3.79*		-6.06*	-2.30*
Loam	-36.53	-21.90*	Clay	-26.89	-27.12
	-9.73	-9.44*		-7.71	-6.51
	-1.60	-3.45*		-1.46	-14.06
					-1.24
Clay	-18.27	-10.05	Sand	-0.322*	-0.253*
	-5.69	-5.23			
	-3.48	-2.28			
		-1.04			

*Fit by eye; all others fit by regression.

All digits shown are significant.

All slopes have dimensions of 1/hr.

Gardner (1963).

Based on these criteria and by comparison of the slopes of the line segments from experiments one, two, and three, the line segments in the plot of data from experiment four (Figure 5) were assigned to soil layers as shown in Table 2. There were four line segments in the loam layer, four line segments in the clay layer, and one line segment in the sand layer. The break in data from 0.091 hours to 0.107 hours in the loam layer occurred when the flow was changed to the lower reading flow meter.

DISCUSSION

I have found nothing in the literature to suggest the occurrence of line segments within a soil layer. To aid in determining the validity of the hypothesis of the line segment model of infiltration a computer program was developed.[1]

The program fits three straight lines through n points. The sum of the error from the linear least square regressions is minimized. The error for one line through n points may be expressed by:

$$E = \left(\int_{\alpha}^{\beta} (Y - mx - b)^2 \, dx \right)^{\frac{1}{2}}$$

Taking the partial derivative of E with respect to m (the slope) and b (the y intercept) gives two equations and two unknowns. These can be solved for m and b. I make use of the independent transformation:

$$x = ((\beta-\alpha)/2)\ u + (\beta+\alpha)/2$$

[1] Consultation with Gary J. Burgess, Graduate Assistant, Department of Mechanics, Metals, and Materials Science, College of Engineering, Michigan State University, East Lansing, Michigan 48824.

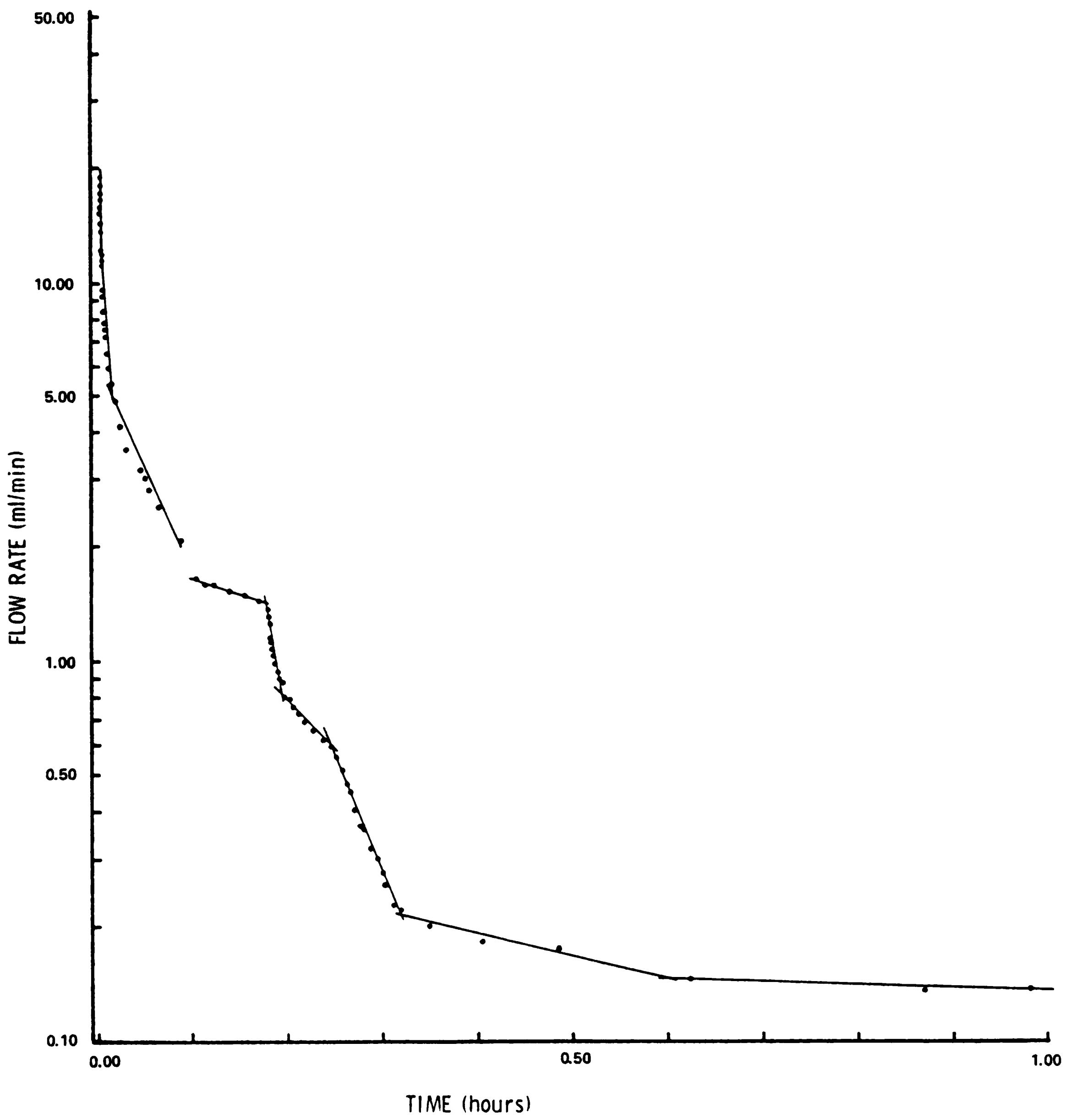

Figure 5. Semi-logarithmic plot from experiment 4.

$$m = (3/(\beta-\alpha)) \int_{-1}^{1} u\ y\ du$$

$$b = \tfrac{1}{2} \int_{-1}^{1} y\ du - (3(\beta+\alpha))/(2(\beta-\alpha)) \int_{-1}^{1} u\ y\ du.$$

For three lines through n points the error is:

$$E = \sum_{i=1}^{3} \left(\int_{\alpha_i}^{\alpha_{i+1}} (Y - m_i x - b_i)^2\ dx \right)$$

m and b may be expressed by Gaussian quadrature formulas, where m and b are fractions of α and β. E can now be expressed:

$$E = \sum_{i=1}^{3} \int_{\alpha_i}^{\alpha_{i+1}} (Y_i - M(\alpha_i, \alpha_{i+1})\ x - b(\alpha_i, \alpha_{i+1})^2\ dx.$$

A computer solves this equation by iteration, fitting the points consisting of the natural logarithm of flow rate and time. The computer program returns for each line segment the number of points, the slope, intercept, and square root of error. The program also computes the sum of the square root of error for three line segments. Only data that appeared to be continuous (no breaks in data) and contain at least three line segments, was fit using the computer program.

A splined fit was used when more than three line segments were suspected. The data was fit to obtain three line segments. The data excluding the points for the first line segment were then fit to obtain three line segments from the remaining data. By comparing the summation of error for three and four line segments, the proper number of line segments could be determined.

The data was fit to three additional curve types, representing existing infiltration models. These curve types were hyperbolic, exponential with asymtote equal to zero, and exponential curves with asymtote not zero. The asymtote obtained from the hyperbolic fit was used as an approximation of the asymtote for the exponential fit. In all but two cases, the hyperbolic fit produced a usable asymtote, i.e., a value less than the smallest data point. For experiment one, the sand layer, and experiment four, the loam layer, a value one tenth less than the smallest flow rate was used as the asymtotic value. The appendix contains copies of the computer programs, data, and results. Table 3 is a summary of results from the different types of curve fitting.

In all cases, the line segment fit produces less error than the other three methods.

The modeling of infiltration using line segments which I propose appears to encompass Bodman and Colman's (1944) classification of zones within an infiltrated layer, and the components of water potential; matrix, pressure, and gravitational potential.

In experiment one, three line segments were identified in each soil layer. I propose the first line segments in these layers is caused by a gradient which is predominantly due to matrix potential. The steep gradient across the wetting front described by Philip (1957) causes high velocities. As the wet front advances, a thin layer of saturated flow is rapidly established at the surface of the soil. The thin saturated layer has two effects. First, the steep gradient across the wetting front is decreased, and second, the saturated layer offers additional resistance to flow and the effects of the matrix potential are damped. Below the saturated zone, a transmission zone is established. The saturated zone advances much more slowly than does the transmission zone.

Table 3. Comparison of error by several curve fitting methods.

	Line Segment	Hyperbolic	Exponential	Exponential and Asymtote
Exp 1				
Sand	0.177 (3 lines)	0.857	12.8	7.13
Loam	0.126 (3 lines)	0.213	3.63	3.35
Clay	0.126 (3 lines)	0.177	1.15	1.026
Exp 2				
Clay	0.164 (4 lines)	0.534	1.27	1.23
Exp 3				
Clay	0.143 (3 lines)	0.264	0.824	0.752
Exp 4				
Loam	0.347 (3 lines)	0.624	16.9	14.02
Clay	0.338 (4 lines)	0.718	1.109	1.07

The soil moisture content in the transmission zone has been shown by Bodman and Colman (1944) to remain relatively constant, the absolute moisture content being dependent on soil texture. A constant moisture content implies that the water potential in the transmission zone remains constant. As the transmission zone lengthens, the gradient causing flow decreases, causing a gradual decrease in the rate of infiltration. The second line segment reflects this as a further dampening of matrix potential, and dissipation of the pressure potential due to an increased resistance because of the increased length of flow path. After some time, frictional dissipation due to increased flow length becomes equal to matrix and pressure potentials, leaving gravitational potential as the predominant driving force. Gravitational potential acts equally over the entire length of the soil column. The third line segment reflects gravitational potential as the remaining influence controlling the rate of water entry into the soil since matrix and pressure potentials have been damped by friction.

Increasing the head causing flow in experiment two resulted in an increase of pressure potential. The increase in pressure potential increased the total potential, and therefore the gradient, in the transmission zone. This caused a shift of the second line segment within the sand layer resulting in a fourth line segment. The loam layer in experiment two conforms to the proposed hypothesis.

Four line segments are shown in the clay layer of experiment two. The break in slope between the first and second line segments coincides with the time the wet front passed the discontinuity in the clay layer. The remaining line segments in the clay layer occur as hypothesized above.

Experiments three and four generally fit the hypothesis as proposed. In experiment three, the third line segment in the loam layer, I believe, is a continuation of the second line segment. Flow was switched at this time to another flow meter to maintain measuring capability. Due to lack of calibration of the flow meters the slopes do not match. The clay layer in experiment three contains three line segments as expected.

Experiment four was similar to experiment three. The fourth line segment in the loam layer, I believe, is an extension of the third line segment, again the slopes do not match due to a change of flow meters. I cannot explain the anomaly in the clay layer. I believe there was a discontinuity due to differential packing or stratification when the soil column was filled.

Looking at Figure 2, the graph of experiment one, the data would appear to fit one exponential curve very well, with the exception of the points in the vicinity of the soil layer interfaces. If there were fewer data points than were provided by the recording method used, the points in the vicinity of the soil layer interfaces might be considered "acceptable scatter". The linearity might not be as obvious and the data would be fit as in the past to some type of exponential curve.

Using line segments to fit infiltration data provides a good fit of the data over the entire range of time, whereas the classical models fit the data well only in certain ranges of time.

V. SUMMARY AND CONCLUSIONS

SUMMARY

Vertical infiltration tests using a constant head device were run using layered, air dry soil in a glass column. Two experimental runs used soil layers of sand, loam and clay from top to bottom. Loam, clay and sand layers were used from top to bottom in the remaining two experiments.

A video cassette recording system was used to record instantaneous volume flow rate and time from a digital timer and variable area flow meter. The recording system provided the potential for 3600 data points per minute.

It was found when the data were plotted with the logarithm of volume flow rate on the vertical axis and time on the horizontal axis, the infiltration curve was represented by a series of line segments. Several of these line segments would represent the flow within a soil layer. Repeatable breaks occurred at times corresponding to the passage of the visible wet front at an interface between soil layers.

A literature review was conducted and none of the infiltration equations for homogeneous soil suggested the occurrence of line segments within a soil layer. The literature review did, however, produce evidence which supports the interpretation that breaks in the slope of infiltration curves is due to the passage of the wet front into a different textured soil layer (Colman and Bodman (1945) and Miller and Gardner (1962)).

CONCLUSIONS

From the research conducted I conclude:

1. A wet front passing an interface between two texturally different layers can be detected in infiltration data.
2. The data will enable one to determine if the wet front passed into a finer or a coarser soil layer.
3. The line segments of a graph of infiltration data within a soil layer are, to some extent, affected by the preceding layer.
4. The model of infiltration best fitting the observed data as fit by least square error is comprised of three straight line segments.
5. The straight line segments can be related to components of the total water potential specifically, matrix potential, pressure potential, and gravitational potential.

VI. SUGGESTIONS FOR FUTURE CONSIDERATION

The following are suggestions for the improvement of measurement techniques for additional experiments to investigate the proposed hypothesis.

A flow meter with smaller divisions over the range of flow rates measured should be used. More divisions would increase the number of data points available for analysis as well as the accuracy in reading the data.

There are two experiments that would also be useful. A long soil column with one homogeneous soil layer should be used for each. In the first experiment the soil column should be maintained vertically. The experiment should be long enough in duration to insure that flow would be influenced by the gravitational component only. At this time the pressure head should be increased a predetermined amount. The increased head should produce two line segments in addition to the first three line segments. The slope of the fourth line segment should be steeper than the third line segment. The difference between the pressure potential line segments should be found to be directly proportional to the head increase. The two additional line segments model the influence of flow as a function of increase in pressure potential. When the frictional losses balance the higher pressure potential, the fifth line segment will model flow due to the influence of gravitational potential. The slope of the fifth line segment should be very close to the slope of the third line segment.

The second experiment should be run with the soil column horizontal. A horizontal position should eliminate the line segment due to gravitational potential. After the flow decreases and approaches zero, if the head is increased a third line segment should be produced. Again the difference in slopes between the second and third line segment will be directly proportional to the increase in head. No fourth or fifth line segment should appear.

LIST OF REFERENCES

LIST OF REFERENCES

Barnes, B. S., 1940. Discussion of analysis of runoff characteristics. Trans., ASCA, Vol. 105, p. 106.

Bodman, G. B. and E. A. Coleman. 1944. Moisture and energy conditions of water into soils. Soil Sci. Soc. of Amer. Proc., 8:116-122.

Buckingham, E. 1907. USDA Bureau of soils. Bull. #38. A 26.3:38.

Childs, E. C. and M. Bybordi. 1969. The vertical movement of water in stratified porous material, 1, Infiltration. Water Resources Res., 5(2):445-459.

Collis-George, N. 1974. A laboratory study of infiltration-Advance. Soil Sci., 117(5), 283-287.

Collis-George, N. 1977. Infiltration equations for simple soil systems. Water Resources Research, Vol 13, No. 2.

Coleman, E. A. and G. B. Bodman. 1945. Moisture and energy conditions during downward entry of water into moist and layered soils. Soil Sci. Soc. of Amer. Proc., 9:3-11.

Gardner, W. R. 1967. Development of the modern infiltration theory and application in hydrology. Trans. of ASAE, 10(3):379-381.

Gardner, W. R. and J. A. Widstoe. 1921.The movement of soil moisture, Soil Sci., 11:215-232.

Green, W. H. and G. A. Ampt. 1911. The flow of air and water through soils. Journal Agricultural Science, 4(1):1-24.

Holtan, H. N. 1961. A concept for infiltration estimates in watershed engineering. USDA Res. Serv. ARS:41-51.

Horton, R. E. 1937. Hydrologic Interelation of water and soil. Soil Sci. Soc. of Amer. Proc., 1:401-429.

Horton, R. E. 1940. An approach toward the physical interpretation of infiltration capacity. Soil Sci. Soc. of Amer. Proc., 5:399-417.

Idike, F. I. 1977. Experimental evaluation of infiltration equations. Unpublished MS Thesis, Agricultural Engineering Department, University of Minnesota, St. Paul.

Kostiakov, A. N. 1932. Dynamics of the infiltration coefficient of water into the subsoil and the need for a dynamic approach to the study of it for soil reclemation pruposes. Trans. Sixth Comm. Intern. Soc. Soil Sci. Russian PT. A. 17-21.

Miller, D. E. and W. H. Gardner. 1962. Water infiltration into stratified soil. Soil Sci. Soc. of Amer. Proc., 26:115-119.

Musgrave, G. W. and G. R. Free. 1936. Factors that modify the rate and total amount of soil infiltration. Amer. Soc. Agron Jour., 28:727-739.

Mein, R. G. and C. L. Larson. 1971. Modeling the infiltration component of the rainfall-runoff process. Minnesota Water Resources Research Center Full #43. University of Minnesota. Minneapolis, Minnesota.

Overton, D. E. 1964. Mathematical refinement of an infiltration equation for watershed engineering. USDA, Ag. Res. Ser., ARS. 41-99.

Philip, J. R. 1954. An infiltration equation with physical significance. Soil Sci., 77-153.

Philip, J. R. 1957. The theory of infiltration, 4, Sorptivity and algebraic infiltration equations. Soil Sci., 84(3):257-264.

Philip, J. R. 1957. The theory of infiltration Pt. 3. Soil Sci., 84: 163-178.

Richards, L. A. 1931. Capillary conduction through porous mediums. Physics I:318-333.

Skaggs, R. W., L. F. Huggins, E. J. Monke, and G. R. Foster. 1969. Experimental evaluation of infiltration equations. Trans. Am. Soc. Agric. Eng., 12(6):822-828.

Smith, R. E. 1975. Approximations for vertical infiltration rate patterns. Paper 75-2010 ASAE. Presented Davis, California.

Swartzendruber, D. 1966. Soil water behavior as described by transport coefficients and functions. Advances in Agronomy, 18:327-370.

Swartzendruber, D., and M. R. Huberty. 1958. Use of infiltration equation parameters to evaluate infiltration difference in the field. Trans. Am. Geophy. Union, 39:84-93.

Watson, K. K. 1959. A note on the field use of a theoretically derived infiltration equation. Jour. Geophys. Res. 64:1611-1615.

Taylor, S. A. and G. L. Ashcroft. 1972. Physical Edaphology. W. H. Freeman and Company, San Francisco.

APPENDICES

APPENDIX A

FLOW METER CALIBRATION CHARTS

APPENDIX A

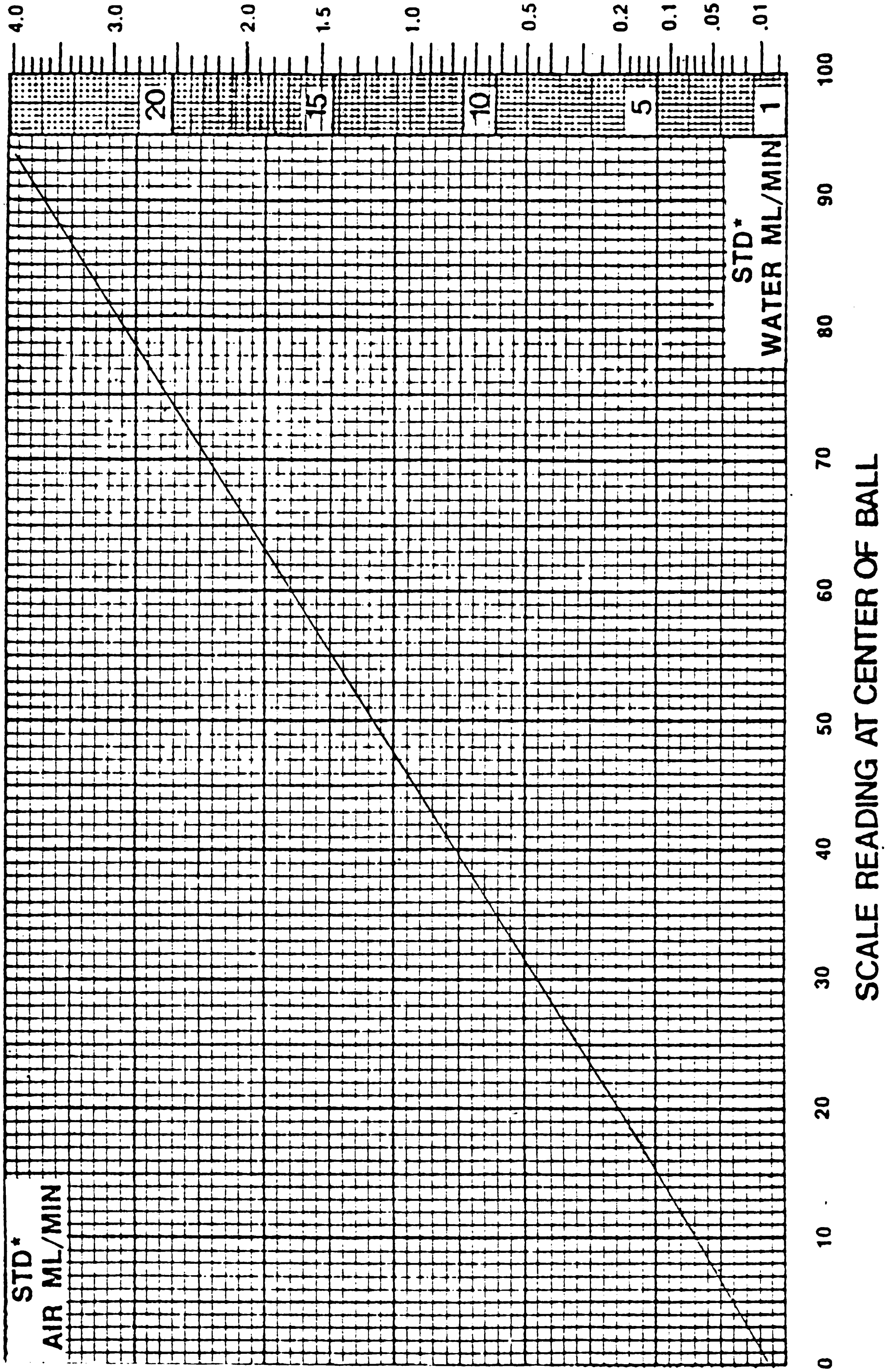

Figure 6. Calibration chart for Gilmont flow meter.

APPENDIX A

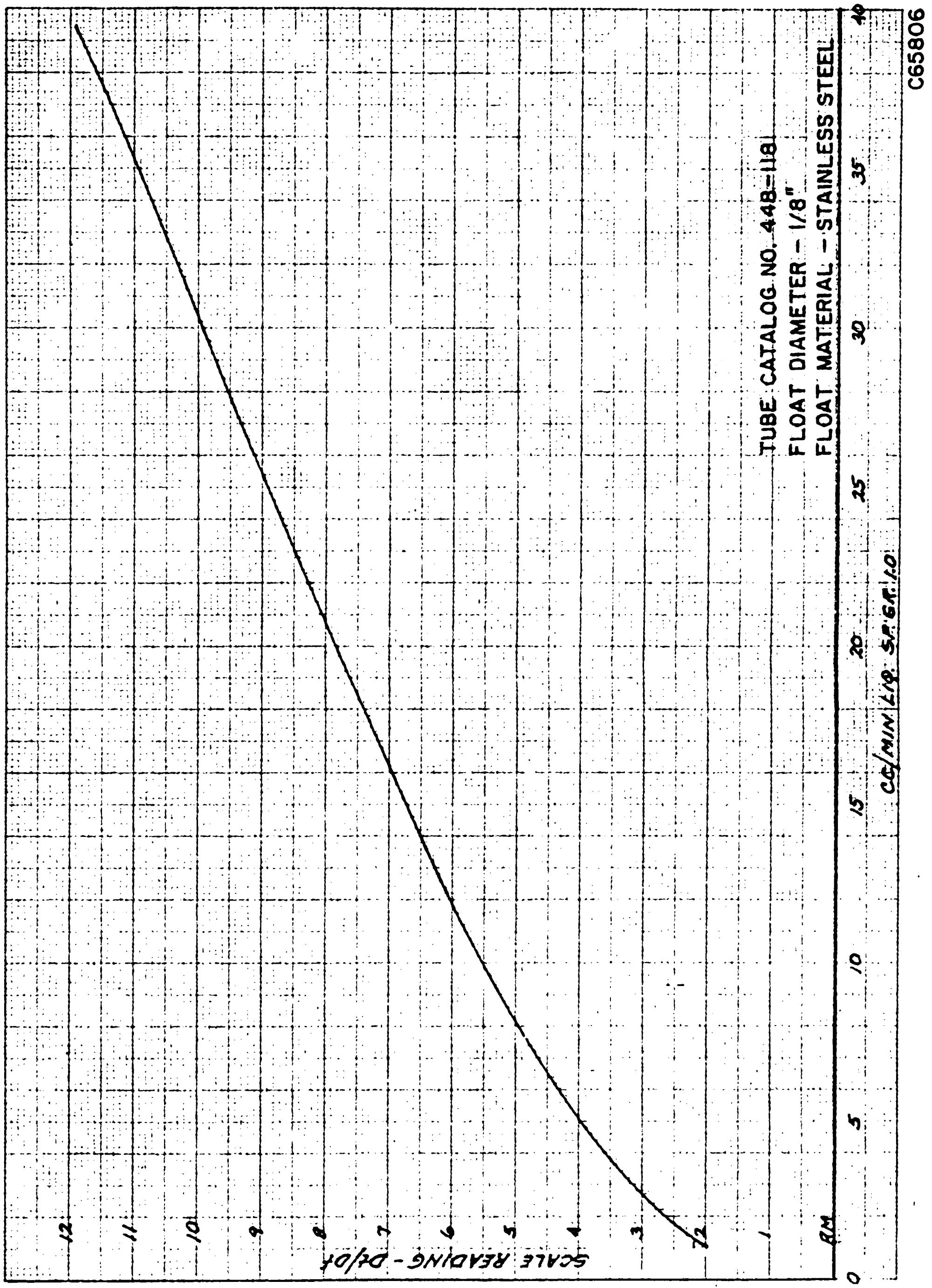

Figure 7. Calibration chart for Fischer-Porter flow meter.

APPENDIX B

EXPERIMENTAL DATA

APPENDIX B

TABLE 4. DATA FROM EXPERIMENT ONE.

TIME (MIN-SEC)	DECIMAL (1) TIME(HRS.)	FLOW (2) (ML/MIN)	FLOW TUBE READING
0.15	0.0000416	5.60	4.20
0.45	0.0001250	11.80	6.00
.062	0.0001722	14.00	6.50
0.75	0.0002083	16.20	7.00
1.15	0.0003194	20.70	8.00
1.82	0.0005055	25.40	9.00
2.53	0.0007027	27.80	9.50
4.69	0.0013030	27.80	9.50
9.29	0.0025810	27.80	9.50
10.03	0.0027860	27.30	9.40
15.79	0.0043860	23.00	8.50
21.15	0.0058750	20.70	8.00
30.76	0.0085440	18.40	7.50
37.59	0.0104420	16.20	7.00
57.52	0.0159800	14.80	6.70
1:06.36	0.0184300	14.00	6.50
1:23.25	0.0231300	14.00	6.50
1:33.39	0.0259400	12.60	6.20
2:12.69	0.0368600	12.50	6.15
2:57.62	0.0433400	12.20	6.10
3:29.78	0.0582700	11.80	6.00
3:36.89	0.0602470	11.40	5.90
3:40.36	0.0612100	10.90	5.75
3:44.65	0.0624030	9.90	5.50
3:47.86	0.0632900	9.70	5.45
3:58.82	0.0663400	9.00	5.25
4:04.32	0.0678700	8.40	5.15
4:14.66	0.0707390	8.10	5.00
4:28.29	0.0745300	7.80	4.80
4:59.56	0.0832100	6.80	4.60
5:44.78	0.0957700	6.60	4.40
6:32.26	0.1089600	5.50	4.30
7:25.29	0.1237000	5.40	4.20
9:24.96	0.1569000	5.10	4.00
10:56.25	0.1823000	4.50	3.80
11:13.05	0.1870000	4.00	3.60
11:35.56	0.1932000	3.70	3.40
12:07.18	0.2019900	3.10	3.20
12:56.95	0.2158000	2.70	3.00
14:55.96	0.2489000	2.30	2.80
16:37.43	0.2771000	2.10	2.60
17:43.19	0.2953000	1.70	2.50
18:53.89	0.3150000	1.60	2.40
22:16.22	0.3712000	1.30	2.20
26:58.49	0.4496000	1.00	2.00

1. ACCURATE TO FOUR SIGNIFICANT DIGITS.
2. ACCURATE TO THREE SIGNIFICANT DIGITS.

APPENDIX B

TABLE 5. DATA FROM EXPERIMENT TWO.

TIME (MIN-SEC)	DECIMAL (1) TIME(HRS.)	FLOW (2) (ML/MIN)	FLOW TUBE READING
00:04.98	0.0013830	14.60	6.40
00:08.99	0.0024970	11.80	6.00
00:10.38	0.0028830	9.90	5.50
00:12.58	0.0034940	8.40	5.10
00:14.48	0.0040222	8.10	5.00
00:20.18	0.0056056	7.50	4.80
00:36.69	0.0101920	6.80	4.60
01:06.68	0.0185200	6.50	4.50
01:17.58	0.0215500	6.20	4.40
01:42.68	0.0285200	5.70	4.20
02:05.38	0.0348300	5.00	4.00
02:42.28	0.0450800	5.70	4.20
02:42.98	0.0452700	6.20	4.40
02:45.49	0.0459700	6.80	4.60
02:46.88	0.0463600	7.10	4.70
03:23.08	0.0546100	6.80	4.60
04:23.58	0.0732200	6.50	4.50
08:15.69	0.1377000	6.20	4.40
09:25.98	0.1572000	5.90	4.30
09:32.78	0.1591000	5.70	4.20
09:45.06	0.1625000	5.00	4.00
10:12.79	0.1702000	4.50	3.80
10:48.29	0.1800810	4.00	3.60
11:47.98	0.1967000	3.50	3.40
13:14.68	0.2207000	2.23	69.50
13:19.38	0.2221000	2.30	70.50
13:31.68	0.2255000	2.25	70.00
13:55.16	0.2320000	2.20	69.00
14:16.45	0.2379000	2.13	68.00
14:53.98	0.2483000	2.08	67.00
15:21.95	0.2561000	1.98	65.00
16:07.09	0.2686000	1.90	64.00
16:39.15	0.2775000	1.85	63.00
17:14.05	0.2873000	1.78	62.00
18:21.22	0.3059000	1.70	61.00
20:15.62	0.3377000	1.68	60.00
20:51.25	0.3476000	2.33	71.00
21:42.09	0.3617000	2.08	67.00
21:49.36	0.3637000	1.95	65.00
22:00.88	0.3669000	1.85	63.00
22:05.49	0.3682000	1.75	62.00
22:12.09	0.3700000	1.70	61.00
22:53.92	0.3816000	1.63	59.00
23:01.88	0.3839000	1.58	58.00
23:21.56	0.3893000	1.52	57.00

1. ACCURATE TO FOUR SIGNIFICANT DIGITS.
2. ACCURATE TO THREE SIGNIFICANT DIGITS.

APPENDIX B

TABLE 5. (CONT'D.)

TIME (MIN-SEC)	DECIMAL (1) TIME(HRS.)	FLOW (2) (ML/MIN)	FLOW TUBE READING
23:39.09	0.3942000	1.42	55.00
23:53.49	0.3982000	1.35	54.00
24:03.58	0.4010000	1.33	53.00
24:19.13	0.4053000	1.30	52.00
24:31.19	0.4087000	1.23	51.00
24:46.25	0.4128000	1.20	50.00
25:11.59	0.4199000	1.16	49.00
25:40.59	0.4279000	1.10	48.00
26:10.09	0.4361000	1.08	47.00
26:46.29	0.4462000	1.00	46.00
27:29.39	0.4582000	0.95	45.00
28:36.59	0.4768000	0.93	44.00
29:25.45	0.4904000	0.88	43.00
30:36.19	0.5101000	0.85	42.00
32:09.55	0.5360000	0.80	41.00
34:18.75	0.5719000	0.78	40.00
36:36.63	0.6102000	0.75	39.00
39:34.79	0.6597000	0.70	38.00
42:26.32	0.7073000	0.67	37.00
49:10.58	0.8196000	0.60	35.00

1. ACCURATE TO FOUR SIGNIFICANT DIGITS.
2. ACCURATE TO THREE SIGNIFICANT DIGITS.

APPENDIX B

TABLE 6. DATA FROM EXPERIMENT THREE.

TIME (MIN-SEC)	DECIMAL (1) TIME(HRS.)	FLOW (2) (ML/MIN)	FLOW TUBE READING
00:09.19	0.0025530	11.80	6.00
00:11.99	0.0033310	9.90	5.50
00:17.00	0.0047220	8.10	5.00
00:21.98	0.0061060	7.50	4.80
00:33.05	0.0091810	6.20	4.40
00:43.09	0.0119700	5.60	4.20
00:55.39	0.0153900	5.00	4.00
01:26.49	0.0240300	2.50	74.00
01:37.45	0.0270700	2.40	73.00
01:54.19	0.0317200	2.30	71.00
02:02.49	0.0340300	2.25	70.00
02:14.48	0.0373600	2.20	69.00
02:22.55	0.0396000	2.12	68.00
02:40.09	0.0444700	2.09	67.00
02:54.98	0.0446100	2.05	66.00
03.13.69	0.0538000	1.95	65.00
03:35.79	0.0599400	1.90	64.00
03:50.09	0.0639100	1.85	63.00
04:26.08	0.0739100	1.74	61.00
04:35.24	0.0764600	1.68	60.00
04:47.69	0.0799100	1.58	58.00
04:52.08	0.0811300	1.50	57.00
04:56.48	0.0795800	1.45	56.00
04:58.46	0.0829100	1.40	55.00
05:00.19	0.0833900	1.38	54.00
05:02.44	0.0840100	1.34	53.00
05:06.00	0.0850000	1.30	52.00
05:15.18	0.0875300	1.24	51.00
05:26.49	0.0906900	1.20	50.00
05:45.26	0.0995100	1.16	49.00
06:02.54	0.1007000	1.10	48.00
06:19.80	0.1055000	1.06	47.00
06:32.39	0.1089000	1.00	46.00
06:54.59	0.1152000	0.96	45.00
07:29.98	0.1250000	0.94	44.00
08:04.59	0.1346000	0.86	43.00
08:58.39	0.1496000	0.85	42.00
10:11.34	0.1698000	0.81	41.00
11:42.59	0.1952000	0.78	40.00
13:33.59	0.2260000	0.74	39.00
16:07.55	0.2688000	0.70	38.00
19:18.69	0.3219000	0.66	37.00
23:59.69	0.3999000	0.64	36.00
30:00.00	0.5000000	0.62	35.00

1. ACCURATE TO FOUR SIGNIFICANT DIGITS.
2. ACCURATE TO THREE SIGNIFICANT DIGITS.

APPENDIX B

TABLE 7. DATA FROM EXPERIMENT FOUR.

TIME (MIN-SEC)	DECIMAL (1) TIME(HRS.)	FLOW (2) (ML/MIN)	FLOW TUBE READING
00:00.05	0.0000138	8.10	5.00
00:17.60	0.0048890	19.40	7.70
00:17.99	0.0049970	18.40	7.50
00:18.45	0.0051250	17.60	7.30
00:18.89	0.0052670	17.10	7.20
00:19.59	0.0054420	16.20	7.00
00:19.88	0.0055220	15.80	6.90
00:20.65	0.0057360	14.80	6.70
00:21.49	0.0059690	14.00	6.50
00:23.69	0.0065810	12.60	6.20
00:24.49	0.0068030	12.20	6.10
00:25.09	0.0069690	11.80	6.00
00:25.79	0.0071640	11.40	5.90
00:29.65	0.0082360	9.90	5.50
00:32.00	0.0088890	9.60	5.40
00:34.65	0.0096250	8.80	5.20
00:37.79	0.0105000	8.20	5.00
00:41.79	0.0116100	7.80	4.90
00:43.59	0.0121100	7.50	4.80
00:47.89	0.0133000	6.80	4.60
00:52.96	0.0147100	6.20	4.40
01:01.29	0.0170300	5.60	4.20
00:15.09	0.0208600	5.10	4.00
01:34.29	0.0261900	4.40	3.70
01:56.59	0.0323900	3.80	3.50
02:53.98	0.0483300	3.40	3.40
03:14.03	0.0539000	3.20	3.25
03:26.63	0.0574000	3.00	3.15
04:00.69	0.0668600	2.70	3.00
05:27.68	0.0910200	2.20	2.75
06:23.69	0.1066000	1.75	61.50
06:54.29	0.1151000	1.70	60.50
07:28.43	0.1246000	1.68	60.00
08:30.90	0.1419000	1.63	59.00
09:29.48	0.1582000	1.58	58.00
10:27.49	0.1743000	1.53	57.00
10:55.78	0.1822000	1.45	56.00
10:57.48	0.1826000	1.40	55.00
11:00.09	0.1834000	1.34	53.00
11:03.98	0.1844000	1.22	51.00
11:06.39	0.1851000	1.20	50.00
11:11.00	0.1864000	1.15	49.00
11:15.59	0.1877000	1.10	48.00
11:22.79	0.1897000	1.06	47.00
11:29.98	0.1917000	1.00	46.00

1. ACCURATE TO FOUR SIGNIFICANT DIGITS.
2. ACCURATE TO THREE SIGNIFICANT DIGITS.

APPENDIX B

TABLE 7. (CONT'D.)

TIME (MIN-SEC)	DECIMAL (1) TIME(HRS.)	FLOW (2) (ML/MIN)	FLOW TUBE READING
11:49.85	0.1972000	0.94	44.00
11:59.49	0.1999000	0.86	43.00
12:13.69	0.2038000	0.85	42.00
12:25.29	0.2070000	0.81	41.00
12:46.48	0.2129000	0.78	40.00
13:10.29	0.2195000	0.74	39.00
13:41.19	0.2281000	0.70	38.00
14:21.99	0.2394000	0.66	37.00
14:48.82	0.2469000	0.64	36.00
15:10.69	0.2530000	0.60	35.00
15:32.79	0.2591000	0.55	33.00
15:48.29	0.2634000	0.51	32.00
16:05.78	0.2683000	0.49	31.00
16:22.08	0.2728000	0.44	30.00
16:37.00	0.2769000	0.40	29.00
16:55.69	0.2821000	0.39	28.00
17:16.19	0.2878000	0.35	27.00
17:40.53	0.2956000	0.33	26.00
18:06.29	0.3017000	0.30	25.00
18:32.19	0.3039000	0.28	24.00
18:46.43	0.3129000	0.25	23.00
19:11.93	0.3200000	0.24	22.00
21:01.00	0.3503000	0.22	21.00
24:24.41	0.4068000	0.20	20.00
29:14.72	0.4874000	0.19	19.00
37:28.49	0.6246000	0.16	18.00
52:15.98	0.8711000	0.15	17.00
58:56.17	0.9823000	0.15	17.00

1. ACCURATE TO FOUR SIGNIFICANT DIGITS.
2. ACCURATE TO THREE SIGNIFICANT DIGITS.

APPENDIX C

COMPUTER PROGRAMS

APPENDIX C

```
10 REM THIS PROGRAM FITS A HYPERBOLIC CURVE
20 DIM C(100),D(100),X(100),Y(100),Y1(100)
25 FILES TEST
30 PRINT "NUMBER OF RECORDS TO BE READ"
40 INPUT Z
50 RESTORE
60 FOR I = 1 TO Z
70 READ #1,C(I),D(I)
80 NEXT I
85 RESTORE
90 PRINT "NUMBER OF RECORDS USED? START WITH RECORD?"
100 INPUT N,Z2
110 FOR I = 1 TO N
120 X(I)=C(I+Z2)
130 Y(I)=D(I+Z2)
140 Y1(I)=LOG(D(I+Z2))
150 PRINT X(I),Y(I)
160 NEXT I
170 S1=S2=S3=S4=S5=0
180 FOR I = 1 TO N
190 S1=S1+(1/X(I))
200 S2=S2+Y1(I)
210 S3=S3+(1/X(I))**2
220 S4=S4+Y1(I)**2
230 S5=S5+(1/X(I))*Y1(I)
240 NEXT I
250 B=(N*S5-S2*S1)/(N*S3-S1**2)
260 A=(S2-B*S1)/N
270 E=0
280 FOR I = 1 TO N
290 E=E+(Y1(I)-(B/X(I))-A)**2
300 NEXT I
310 PRINT
320 PRINT
330 PRINT "ERROR =" SQR(E)
340 PRINT "LOG OF ASYMTOTE =" A
350 PRINT "SLOPE    =" B
360 A1=EXP(A)
370 PRINT "ASYMTOTE ="A1
380 PRINT TAB(7),"FLOW - ASYMTOTE"
390 FOR I = 1 TO N
400 PRINT Y(I)-A1
410 NEXT I
420 PRINT "ANOTHER RUN? 1=YES."
430 INPUT Q
440 IF Q=1 THEN 90
450 END
```

Figure 8. Program for fitting hyperbolic curves.

APPENDIX C

```
10 REM THIS PROGRAM FITS A EXPONENTIAL CURVE
20 DIM C(100),D(100),X(100),Y(100),Y1(100)
25 FILES TEST
30 PRINT "NUMBER OF RECORDS TO BE READ"
40 INPUT Z
50 RESTORE
60 FOR I = 1 TO Z
70 READ #1,C(I),D(I)
80 NEXT I
85 RESTORE
90 PRINT "NUMBER OF RECORDS USED? START WITH RECORD?"
100 INPUT N,Z2
105 PRINT "ENTER ASYMTOTE"
107 INPUT B1
110 FOR I = 1 TO N
120 X(I)=C(I+Z2)
130 Y(I)=D(I+Z2)-B1
140 Y1(I)=LOG(Y(I))
150 PRINT X(I),D(I+Z2),Y1(I)
160 NEXT I
170 S1=S2=S3=S4=S5=0
180 FOR I = 1 TO N
190 S1=S1+(X(I))
200 S2=S2+Y1(I)
210 S3=S3+(X(I))**2
220 S4=S4+Y1(I)**2
230 S5=S5+(X(I))*Y1(I)
240 NEXT I
250 B=(N*S5-S2*S1)/(N*S3-S1**2)
260 A=(S2/N)-(B*(S1/N))
270 E=0
280 FOR I = 1 TO N
290 E=E+(Y(I)-(EXP(A)*EXP(B*X(I))))**2
300 NEXT I
310 PRINT
320 PRINT
330 PRINT "ERROR =" SQR(E)
340 PRINT "INTERCEPT ="EXP(A)
350 PRINT "SLOPE     =" B
351 PRINT "ASYMTOTE ="B1
352 PRINT
353 PRINT
354 PRINT
420 PRINT "ANOTHER RUN? 1=YES."
430 INPUT Q
440 IF Q=1 THEN 90
450 END
```

Figure 9. Program for fitting exponential curves.

APPENDIX C

```
10 REM PROGRAM "NBRUT"
20 DIM C(100),D(100),X(100),Y(100)
30 FILES TEST
40 PRINT "NUMBER OF RECORDS TO BE READ"
50 INPUT Z
55 RESTORE
60 FOR I = 1 TO Z
70 READ #1, X(I),Y(I)
80 NEXT I
85 RESTORE
86 PRINT "NUMBER OF RECORDS USED, START WITH RECORD ?"
87 INPUT N,Z2
88 PRINT "DATA POINTS USED"
89 PRINT "  TIME          FLOW"
90 FOR I9 = 1 TO N
100 C(I9)=X(I9+Z2)
200 D(I9)=Y(I9+Z2)
210 PRINT C(I9),D(I9)
220 NEXT I9
230 E0=1000000
240 REM E0 IS WHAT E4 TOTAL ERROR IS COMPARED TO FOR STORAGE
250 FOR N1 = 2 TO N-2
260 L1=1
261 L2=N1
270 GOSUB 520
280 S1=M
281 T1=B
282 E1=SQR(E)
290 FOR N2 = 2 TO N-N1
300 L1=N1
302 L2=N1+N2-1
310 GOSUB 520
320 S2=M
322 T2=B
324 E2=SQR(E)
330 N3=N+2-N1-N2
340 L1=N-N3+1
342 L2=N
350 GOSUB 520
360 S3=M
362 T3=B
364 E3=SQR(E)
370 E4=E1+E2+E3
380 IF E4 > E0 THEN 440
390 E0 = E4
400 R1=N1
402 M1=S1
404 B1=T1
406 E5=E1
```

Figure 10. Program for linear optimization.

APPENDIX C

```
410 R2=N2
412 M2=S2
414 B2=T2
416 E6=E2
420 R3=N3
422 M3=S3
424 B3=T3
426 E7=E3
430 REM R=# POINTS, M=SLOPE, B=Y INTERCEPT, E=SQUARE ERROR
440 REM THIS IS A CONTINUE STATEMENT
450 NEXT N2
460 NEXT N1
462 PRINT"#POINTS            SLOPE          Y INTERCEPT
470 PRINT R1,M1,B1,E5
480 PRINT R2,M2,B2,E6
490 PRINT R3,M3,B3,E7
500 PRINT"SUM OF THE ERROR="E0
502 PRINT "ANOTHER RUN? 1=YES"
504 INPUT Q
506 IF Q=1 THEN 86
510 STOP
520 REM THIS STARTS THE SUBPROGRAM
530 X1=Y1=P1=X2=E=X3=Y3=M=B=0
540 FOR I = L1 TO L2
550 X1=X1+C(I)
555 Y1=Y1+(LOG(D(I)))
570 P1=P1+(C(I)*(LOG(D(I))))
580 X2=X2+(C(I)**2)
590 NEXT I
600 X3=X1/(L2-L1+1)
610 Y3=Y1/(L2-L1+1)
620 M=(P1-(X3*Y1))/(X2-(X3*X1))
630 B=Y3-(M*X3)
640 REM X1=SUM X, Y1=SUM Y, P1= SUM XY, X2=SUM X**2
650 REM X3=X BAR, Y3=Y BAR, M=SLOPE, B=Y INTERCEPT
660 FOR J = L1 TO L2
670 E=E+(LOG(D(J))-(M*C(J))-B)**2
680 NEXT J
690 RETURN
700 REM THIS IS THE END OF THE ENTIRE PROGRAM
710 END
```

Figure 10. (continued)

APPENDIX D

COMPUTER RESULTS

APPENDIX D

0.0007	27.8
0.0013	27.8
0.0026	27.8
0.0028	27.3
0.0044	23
0.0059	20.7
0.0085	18.4
0.0104	16.2
0.016	14.8
0.0184	14
0.0231	14
0.0259	12.6
0.0369	12.5
0.0493	12.2
0.0583	11.8

ERROR = .85657518625
LOG OF ASYMTOTE = 2.7129614229
SLOPE = 6.43063757-4
ASYMTOTE = 15.073849525

Table 8. Hyperbolic curve fitting; experiment one, sand.

0.0583	11.8
0.0602	11.4
0.0612	10.9
0.0624	9.9
0.0633	9.7
0.0663	9
0.0679	8.4
0.0707	8.1
0.0745	7.8
0.0832	6.8
0.0958	6.6
0.109	5.5
0.1237	5.4
0.1569	5.1

ERROR = .21344756094
LOG OF ASYMTOTE = 1.0310245121
SLOPE = .07938007029
ASYMTOTE = 2.8039370312

Table 9. Hyperbolic curve fitting; experiment one, loam.

APPENDIX D

0.1823	4.5
0.187	4
0.1932	3.7
0.202	3.1
0.2158	2.7
0.2489	2.3
0.2771	2.1
0.2953	1.7
0.315	1.6
0.3712	1.3
0.4496	1

ERROR = .17727466348
LOG OF ASYMTOTE =-.90022295176
SLOPE = .42648859065
ASYMTOTE = .40647902442

Table 10. Hyperbolic curve fitting; experiment one, clay.

APPENDIX D

0.3476	2.33
0.3617	2.08
0.3637	1.95
0.3669	1.85
0.3682	1.75
0.37	1.7
0.3816	1.63
0.3839	1.58
0.3893	1.52
0.3922	1.45
0.3942	1.42
0.3982	1.35
0.401	1.33
0.4053	1.3
0.4087	1.23
0.4128	1.2
0.4199	1.16
0.4279	1.1
0.4361	1.08
0.4462	1
0.4582	0.95
0.4768	0.93
0.4904	0.88
0.5101	0.85
0.536	0.8
0.5719	0.78
0.6102	0.75
0.6597	0.7
0.7073	0.67
0.8196	0.6

ERROR = .53444363969
LOG OF ASYMTOTE =-1.6556668776
SLOPE = .79811836194
ASYMTOTE = .19096466318

Table 11. Hyperbolic curve fitting; experiment two, clay.

APPENDIX D

0.07391	1.74
0.07646	1.68
0.07991	1.58
0.08113	1.5
0.0824	1.45
0.08291	1.4
0.08339	1.38
0.08401	1.34
0.085	1.3
0.08753	1.24
0.09069	1.2
0.09591	1.16
0.1007	1.1
0.1055	1.06
0.1089	1
0.1152	0.96
0.125	0.94
0.1346	0.86
0.1496	0.85
0.1698	0.81
0.1952	0.78
0.226	0.74
0.2688	0.7
0.3219	0.66

ERROR = .26369715685
LOG OF ASYMTOTE =-.74495358215
SLOPE = .08922730024
ASYMTOTE = .47475633660

Table 12. Hyperbolic curve fitting; experiment three, clay.

APPENDIX D

0.004889	19.4
0.004997	18.4
0.005125	17.6
0.005267	17.1
0.005442	16.2
0.005522	15.8
0.005736	14.8
0.005969	14
0.006581	12.6
0.006803	12.2
0.006969	11.8
0.007164	11.4
0.008236	9.9
0.008889	9.6
0.009625	8.8
0.0105	8.2
0.01161	7.8
0.01211	7.5
0.0133	6.8
0.01471	6.2
0.01703	5.6
0.02086	5.1
0.02619	4.4
0.03239	3.8
0.04833	3.4
0.0539	3.2
0.0574	3
0.06686	2.7
0.09102	2.2

ERROR = .62355612597
LOG OF ASYMTOTE = 1.0480939673
SLOPE = .00976264201
ASYMTOTE = 2.8522095291

Table 13. Hyperbolic curve fitting; experiment four, loam.

APPENDIX D

0.1822	1.45
0.1826	1.4
0.1834	1.34
0.1844	1.22
0.1851	1.2
0.1864	1.15
0.1877	1.1
0.1897	1.06
0.1917	1
0.1938	0.96
0.1972	0.94
0.1999	0.86
0.2038	0.85
0.207	0.81
0.2129	0.78
0.2195	0.74
0.2281	0.7
0.2394	0.66
0.2469	0.64
0.253	0.6
0.2591	0.55
0.2634	0.51
0.2683	0.49
0.2728	0.44
0.2769	0.4
0.2821	0.39
0.2878	0.35
0.2956	0.33
0.3017	0.3
0.3039	0.28
0.3129	0.25
0.32	0.24
0.3503	0.22
0.4068	0.2
0.4874	0.19
0.6246	0.16

ERROR = .71827413957
LOG OF ASYMTOTE =-3.047901046
SLOPE = .59777236302
ASYMTOTE = .04745843299

Table 14. Hyperbolic curve fitting; experiment four, clay.

APPENDIX D

0.0007	27.8
0.0013	27.8
0.0026	27.8
0.0028	27.3
0.0044	23
0.0059	20.7
0.0085	18.4
0.0104	16.2
0.016	14.8
0.0184	14
0.0231	14
0.0259	12.6
0.0369	12.5
0.0493	12.2
0.0583	11.8

ERROR = 12.763576011
INTERCEPT = 23.443682673
SLOPE =-15.774399153
ASYMTOTE = 0

0.0007	27.8
0.0013	27.8
0.0026	27.8
0.0028	27.3
0.0044	23
0.0059	20.7
0.0085	18.4
0.0104	16.2
0.016	14.8
0.0184	14
0.0231	14
0.0259	12.6
0.0369	12.5
0.0493	12.2
0.0583	11.8

ERROR = 7.1291036854
INTERCEPT = 14.836898012
SLOPE =-82.691239436
ASYMTOTE = 11.7

Table 15. Exponential curve fitting; experiment one, sand.

APPENDIX D

0.0583	11.8
0.0602	11.4
0.0612	10.9
0.0624	9.9
0.0633	9.7
0.0663	9
0.0679	8.4
0.0707	8.1
0.0745	7.8
0.0832	6.8
0.0958	6.6
0.109	5.5
0.1237	5.4
0.1569	5.1

ERROR = 3.6312388316
INTERCEPT = 16.446181038
SLOPE =-8.7136690468
ASYMTOTE = 0

0.0583	11.8
0.0602	11.4
0.0612	10.9
0.0624	9.9
0.0633	9.7
0.0663	9
0.0679	8.4
0.0707	8.1
0.0745	7.8
0.0832	6.8
0.0958	6.6
0.109	5.5
0.1237	5.4
0.1569	5.1

ERROR = 3.3452087860
INTERCEPT = 16.609741181
SLOPE =-14.472031277
ASYMTOTE = 2.8039370312

Table 16. Exponential curve fitting; experiment one, loam.

APPENDIX D

0.1823	4.5
0.187	4
0.1932	3.7
0.202	3.1
0.2158	2.7
0.2489	2.3
0.2771	2.1
0.2953	1.7
0.315	1.6
0.3712	1.3
0.4496	1

ERROR = 1.1454245445
INTERCEPT = 9.897135588
SLOPE =-5.4652066840
ASYMTOTE = 0

0.1823	4.5
0.187	4
0.1932	3.7
0.202	3.1
0.2158	2.7
0.2489	2.3
0.2771	2.1
0.2953	1.7
0.315	1.6
0.3712	1.3
0.4496	1

ERROR = 1.0262336666
INTERCEPT = 11.844979729
SLOPE =-6.9872191316
ASYMTOTE = .40647902442

Table 17. Exponential curve fitting; experiment one, clay.

APPENDIX D

0.3476	2.33
0.3617	2.08
0.3637	1.95
0.3669	1.85
0.3682	1.75
0.37	1.7
0.3816	1.63
0.3839	1.58
0.3893	1.52
0.3922	1.45
0.3942	1.42
0.3982	1.35
0.401	1.33
0.4053	1.3
0.4087	1.23
0.4128	1.2
0.4199	1.16
0.4279	1.1
0.4361	1.08
0.4462	1
0.4582	0.95
0.4768	0.93
0.4904	0.88
0.5101	0.85
0.536	0.8
0.5719	0.78
0.6102	0.75
0.6597	0.7
0.7073	0.67
0.8196	0.6

ERROR = 1.2670373928
INTERCEPT = 4.3064360135
SLOPE =-2.8178639905
ASYMTOTE = 0

Table 18. Exponential curve fitting; experiment two, clay.

APPENDIX D

0.3476	2.33
0.3617	2.08
0.3637	1.95
0.3669	1.85
0.3682	1.75
0.37	1.7
0.3816	1.63
0.3839	1.58
0.3893	1.52
0.3922	1.45
0.3942	1.42
0.3982	1.35
0.401	1.33
0.4053	1.3
0.4087	1.23
0.4128	1.2
0.4199	1.16
0.4279	1.1
0.4361	1.08
0.4462	1
0.4582	0.95
0.4768	0.93
0.4904	0.88
0.5101	0.85
0.536	0.8
0.5719	0.78
0.6102	0.75
0.6597	0.7
0.7073	0.67
0.8196	0.6

ERROR = 1.2299826799
INTERCEPT = 4.8038983440
SLOPE =-3.4744006275
ASYMTOTE = .19096466318

Table 18. (continued)

APPENDIX D

0.07391	1.74
0.07646	1.68
0.07991	1.58
0.08113	1.5
0.0824	1.45
0.08291	1.4
0.08339	1.38
0.08401	1.34
0.085	1.3
0.08753	1.24
0.09069	1.2
0.09591	1.16
0.1007	1.1
0.1055	1.06
0.1089	1
0.1152	0.96
0.125	0.94
0.1346	0.86
0.1496	0.85
0.1698	0.81
0.1952	0.78
0.226	0.74
0.2688	0.7
0.3219	0.66

ERROR = 0.8236937572
INTERCEPT = 1.7731603887
SLOPE =-3.7939746602
ASYMTOTE = 0

Table 19. Exponential curve fitting; experiment three, clay.

APPENDIX D

0.07391	1.74
0.07646	1.68
0.07991	1.58
0.08113	1.5
0.0824	1.45
0.08291	1.4
0.08339	1.38
0.08401	1.34
0.085	1.3
0.08753	1.24
0.09069	1.2
0.09591	1.16
0.1007	1.1
0.1055	1.06
0.1089	1
0.1152	0.96
0.125	0.94
0.1346	0.86
0.1496	0.85
0.1698	0.81
0.1952	0.78
0.226	0.74
0.2688	0.7
0.3219	0.66

ERROR = .75218009412
INTERCEPT = 1.5465755322
SLOPE =-7.6969088398
ASYMTOTE = 0.474756336

Table 19. (continued)

APPENDIX D

0.004889	19.4
0.004997	18.4
0.005125	17.6
0.005267	17.1
0.005442	16.2
0.005522	15.8
0.005736	14.8
0.005969	14
0.006581	12.6
0.006803	12.2
0.006969	11.8
0.007164	11.4
0.008236	9.9
0.008889	9.6
0.009625	8.8
0.0105	8.2
0.01161	7.8
0.01211	7.5
0.0133	6.8
0.01471	6.2
0.01703	5.6
0.02086	5.1
0.02619	4.4
0.03239	3.8
0.04833	3.4
0.0539	3.2
0.0574	3
0.06686	2.7
0.09102	2.2

ERROR = 16.924611593
INTERCEPT = 13.380101739
SLOPE =-25.704532520
ASYMTOTE = 0

Table 20. Exponential curve fitting; experiment four, loam.

APPENDIX D

0.004889	19.4
0.004997	18.4
0.005125	17.6
0.005267	17.1
0.005442	16.2
0.005522	15.8
0.005736	14.8
0.005969	14
0.006581	12.6
0.006803	12.2
0.006969	11.8
0.007164	11.4
0.008236	9.9
0.008889	9.6
0.009625	8.8
0.0105	8.2
0.01161	7.8
0.01211	7.5
0.0133	6.8
0.01471	6.2
0.01703	5.6
0.02086	5.1
0.02619	4.4
0.03239	3.8
0.04833	3.4
0.0539	3.2
0.0574	3
0.06686	2.7
0.09102	2.2

ERROR = 14.021415327
INTERCEPT = 13.656921392
SLOPE =-52.240523346
ASYMTOTE = 2.1

Table 20. (continued)

APPENDIX D

0.1822	1.45
0.1826	1.4
0.1834	1.34
0.1844	1.22
0.1851	1.2
0.1864	1.15
0.1877	1.1
0.1897	1.06
0.1917	1
0.1938	0.96
0.1972	0.94
0.1999	0.86
0.2038	0.85
0.207	0.81
0.2129	0.78
0.2195	0.74
0.2281	0.7
0.2394	0.66
0.2469	0.64
0.253	0.6
0.2591	0.55
0.2634	0.51
0.2683	0.49
0.2728	0.44
0.2769	0.4
0.2821	0.39
0.2878	0.35
0.2956	0.33
0.3017	0.3
0.3039	0.28
0.3129	0.25
0.32	0.24
0.3503	0.22
0.4068	0.2
0.4874	0.19
0.6246	0.16

ERROR = 1.1090307040
INTERCEPT = 2.8120707203
SLOPE =-6.0906335461
ASYMTOTE = 0

Table 21. Exponential curve fitting; experiment four, clay.

APPENDIX D

0.1822	1.45
0.1826	1.4
0.1834	1.34
0.1844	1.22
0.1851	1.2
0.1864	1.15
0.1877	1.1
0.1897	1.06
0.1917	1
0.1938	0.96
0.1972	0.94
0.1999	0.86
0.2038	0.85
0.207	0.81
0.2129	0.78
0.2195	0.74
0.2281	0.7
0.2394	0.66
0.2469	0.64
0.253	0.6
0.2591	0.55
0.2634	0.51
0.2683	0.49
0.2728	0.44
0.2769	0.4
0.2821	0.39
0.2878	0.35
0.2956	0.33
0.3017	0.3
0.3039	0.28
0.3129	0.25
0.32	0.24
0.3503	0.22
0.4068	0.2
0.4874	0.19
0.6246	0.16

ERROR = 1.0742478377
INTERCEPT = 3.1411243140
SLOPE =-6.9386611946
ASYMTOTE = .04745843299

Table 21. (continued)

APPENDIX D

TIME	FLOW
0.0007	27.8
0.0013	27.8
0.0026	27.8
0.0028	27.3
0.0044	23
0.0059	20.7
0.0085	18.4
0.0104	16.2
0.016	14.8
0.0184	14
0.0231	14
0.0259	12.6
0.0369	12.5
0.0493	12.2
0.0583	11.8

#POINTS	SLOPE	Y INTERCEPT	ERROR
8	-60.666091596	3.4206704425	.10761799653
5	-14.417041357	2.9287536751	.05471617265
4	-1.9918484110	2.5920929777	.01469795883

SUM OF THE ERROR= .17703212801

Table 22. Linear fit error optimization; experiment one, sand.

TIME	FLOW
0.0583	11.8
0.0602	11.4
0.0612	10.9
0.0624	9.9
0.0633	9.7
0.0663	9
0.0679	8.4
0.0707	8.1
0.0745	7.8
0.0832	6.8
0.0958	6.6
0.109	5.5
0.1237	5.4
0.1569	5.1

#POINTS	SLOPE	Y INTERCEPT	ERROR
7	-36.526177166	4.6053571549	.05401458522
6	-9.7321591644	2.7766241353	.06799632285
3	-1.6010572142	1.8813864921	.00384382589

SUM OF THE ERROR= .12585473397

Table 23. Linear fit error optimization; experiment one, loam.

APPENDIX D

TIME	FLOW
0.1823	4.5
0.187	4
0.1932	3.7
0.202	3.1
0.2158	2.7
0.2489	2.3
0.2771	2.1
0.2953	1.7
0.315	1.6
0.3712	1.3
0.4496	1

#POINTS	SLOPE	Y INTERCEPT	ERROR
4	-18.270126420	4.8244045843	.02769359797
6	-5.688629798	2.2568053003	.08869193327
3	-3.4826278885	1.5626455498	.00926381702

SUM OF THE ERROR= .12564934826

Table 24. Linear fit error optimization; experiment one, clay.

APPENDIX D

TIME	FLOW
0.3476	2.33
0.3617	2.08
0.3637	1.95
0.3669	1.85
0.3682	1.75
0.37	1.7
0.3816	1.63
0.3839	1.58
0.3893	1.52
0.3922	1.45
0.3942	1.42
0.3982	1.35
0.401	1.33
0.4053	1.3
0.4087	1.23
0.4128	1.2
0.4199	1.16
0.4279	1.1
0.4361	1.08
0.4462	1
0.4582	0.95
0.4768	0.93
0.4904	0.88
0.5101	0.85
0.536	0.8

#POINTS	SLOPE	Y INTERCEPT	ERROR
15	-10.045694488	4.3120024306	.10878682671
7	-5.2299232295	2.3428223705	.02032571910
5	-2.2840307813	1.0015244473	.01869446428

SUM OF THE ERROR= .14780701009

Table 25. Linear fit error optimization; experiment two, clay (splined).

APPENDIX D

TIME	FLOW
0.4087	1.23
0.4128	1.2
0.4199	1.16
0.4279	1.1
0.4361	1.08
0.4462	1
0.4582	0.95
0.4768	0.93
0.4904	0.88
0.5101	0.85
0.536	0.8
0.5719	0.78
0.6102	0.75
0.6597	0.7
0.7073	0.67
0.8196	0.6

#POINTS	SLOPE	Y INTERCEPT	ERROR
7	-5.2299232295	2.3428223705	.02032571910
5	-2.2840307813	1.0015244473	.01869446428
6	-1.0443917406	.34179521870	.01584164408

SUM OF THE ERROR= .05486182746

Table 25. (continued)

APPENDIX D

TIME	FLOW		
0.07391	1.74		
0.07646	1.68		
0.07991	1.58		
0.08113	1.5		
0.0824	1.45		
0.08291	1.4		
0.08339	1.38		
0.08401	1.34		
0.085	1.3		
0.08753	1.24		
0.09069	1.2		
0.09591	1.16		
0.1007	1.1		
0.1055	1.06		
0.1089	1		
0.1152	0.96		
0.125	0.94		
0.1346	0.86		
0.1496	0.85		
0.1698	0.81		
0.1952	0.78		
0.226	0.74		
0.2688	0.7		
0.3219	0.66		
#POINTS	SLOPE	Y INTERCEPT	ERROR
10	-26.893799748	2.5698654977	.06009528107
9	-7.7080230132	.87518635188	.05773611316
7	-1.4609319209	.04225148748	.02503167391

SUM OF THE ERROR= .14286306814

Table 26. Linear fit error optimization; experiment three, clay.

APPENDIX D

TIME	FLOW
0.004889	19.4
0.004997	18.4
0.005125	17.6
0.005267	17.1
0.005442	16.2
0.005522	15.8
0.005736	14.8
0.005969	14
0.006581	12.6
0.006803	12.2
0.006969	11.8
0.007164	11.4
0.008236	9.9
0.008889	9.6
0.009625	8.8
0.0105	8.2
0.01161	7.8
0.01211	7.5
0.0133	6.8
0.01471	6.2
0.01703	5.6
0.02086	5.1
0.02619	4.4
0.03239	3.8
0.04833	3.4
0.0539	3.2
0.0574	3
0.06686	2.7
0.09102	2.2

#POINTS	SLOPE	Y INTERCEPT	ERROR
12	-223.99118955	4.0152889685	.08048368756
10	-71.029941744	2.8838804970	.09231702703
9	-12.228915529	1.8331540955	.17401755546

SUM OF THE ERROR= .34681827004

Table 27. Linear fit error optimization; experiment four, loam.

APPENDIX D

TIME	FLOW
0.1822	1.45
0.1826	1.4
0.1834	1.34
0.1844	1.22
0.1851	1.2
0.1864	1.15
0.1877	1.1
0.1897	1.06
0.1917	1
0.1938	0.96
0.1972	0.94
0.1999	0.86
0.2038	0.85
0.207	0.81
0.2129	0.78
0.2195	0.74
0.2281	0.7
0.2394	0.66
0.2469	0.64
0.253	0.6
0.2591	0.55
0.2634	0.51
0.2683	0.49
0.2728	0.44
0.2769	0.4
0.2821	0.39
0.2878	0.35
0.2956	0.33
0.3017	0.3
0.3039	0.28
0.3129	0.25
0.32	0.24

#POINTS	SLOPE	Y INTERCEPT	ERROR
12	-27.116053239	5.2345962252	.15123704888
8	-6.5108331891	1.1438353171	.03665705502
14	-14.063882632	3.0288729082	.09389813707

SUM OF THE ERROR= .28179224097

Table 28. Linear fit error optimization; experiment four, clay (splined).

APPENDIX D

TIME	FLOW
0.1999	0.86
0.2038	0.85
0.207	0.81
0.2129	0.78
0.2195	0.74
0.2281	0.7
0.2394	0.66
0.2469	0.64
0.253	0.6
0.2591	0.55
0.2634	0.51
0.2683	0.49
0.2728	0.44
0.2769	0.4
0.2821	0.39
0.2878	0.35
0.2956	0.33
0.3017	0.3
0.3039	0.28
0.3129	0.25
0.32	0.24
0.3503	0.22
0.4068	0.2
0.4874	0.19
0.6246	0.16

#POINTS	SLOPE	Y INTERCEPT	ERROR
8	-6.5108331891	1.1438353171	.03665705502
14	-14.063882632	3.0288729082	.09389813707
5	-1.2371999572	-1.0671280490	.05602923666

SUM OF THE ERROR= .18658442875

Table 28. (continued)

MICHIGAN STATE UNIV. LIBRARIES
31293100634090